Enlightening the primordial dark ages

Iarygina, O.

1 Introduction

"I... a universe of atoms, an atom in the universe."

Richard P. Feynman

1.1 The very early universe cosmology

Since ancient times people have been observing the sky and asking philosophical and theological questions: "Where do we come from?", "How was our world created?". From those times science has made a huge progress and nowadays, with the help of precision measurements and observations within the theoretical approaches of modern cosmology, humanity has learned a lot about space-time and our Universe. Below we briefly outline the most important stages of this development, based mainly on Refs. [1–3]. Throughout the introduction we use natural units $\hbar = c = 1$ and the reduced Planck mass defined by $M_{\rm pl} = (8\pi G)^{-1/2}$.

1.1.1 Cosmological ideas prior to inflation

The breakthrough in modern cosmology started from Albert Einstein with the appearance of the Theory of General Relativity in 1915 [5]. It merged the geometry of space-time and the energy-momentum tensor of matter into a single equation, providing an accurate description of gravitation that has been tested and confirmed by many experiments to date. Despite the fact that matter changes the geometry of the space-time, on the very large scales our Universe appears to be flat, homogeneous and isotropic. The most general solution for such universe was found independently by Friedmann, Lemaître, Robertson, Walker (FLRW) [6–10] in the 1920s and 1930s, that is given by the metric

$$ds^2 = -dt^2 + a(t)^2 \left(dr^2 + r^2(d\theta^2 + \sin^2\theta d\phi^2)\right), \tag{1.1}$$

where $a(t)$ is the scale factor which describes the expansion or contraction of the universe. In particular, the expansion rate is parametrised by the Hubble parameter $H(t) \equiv \frac{\dot{a}(t)}{a(t)}$. Historically, Lemaître was the first who in 1927 suggested that the universe could be traced back in time to an originating single point, which he called the "primeval atom". The first attempt to observe the expansion of the universe was done by Slipher [11] in 1912, who noticed the shift of spectral lines of galaxies. However, he did not relate this to the actual expansion of the universe, but rather with "island universes" outside our Milky Way. Much later, Hubble and Humason [12, 13] combined their own galaxy distance measurements with Slipher's measurements of redshifts and found that galaxies are moving away at speeds proportional to their distance. Lemaître understood that this is caused by the expansion of spacetime. Nowadays this velocity-distance relation is called as *the*

Hubble–Lemaître law

$$v \simeq Hd, \tag{1.2}$$

which established the expansion of the universe as a commonly accepted scientific fact.

Now, for the FLRW metric the energy-momentum tensor is of the form of the energy-momentum tensor of a perfect fluid, with a pressure p and energy density ρ. From Einstein equations Friedmann derived the evolution equations for the homogeneous and isotropic case, that are of the following form

$$3M_{\rm pl}^2 H^2 = \rho, \tag{1.3}$$

$$M_{\rm pl}^2 \dot{H} = -\frac{1}{2}\left(\rho + p\right), \tag{1.4}$$

and called *Friedmann equations*. With known p and ρ it is possible to find the corresponding scale factor, which allows us to trace back the expansion history of the universe. Extrapolating the cosmic expansion backwards in time leads to the idea that the Universe had a finite age and started from a hot and dense state, that gave rise to *the hot Big Bang theory*.

In 1948 Gamov [14] suggested that light elements (namely deuterium, helium, and lithium) were produced at the times when the Universe was hot enough for nucleosynthesis, that is now called Big Bang Nucleosynthesis (BBN). As the Universe cooled down due to its expansion, protons and electrons combined to form neutral hydrogen atoms, initiating the recombination epoch. Since Thomson scattering of photons on free electrons was not efficient any more, the universe became transparent to photons and they could travel freely, i.e. decoupled. This thought led Gamov to the realization that some relic radiation should be present since those times, which we call now the cosmic microwave background (CMB). In the same year [15] Alpher and Herman estimated the present day temperature of the relic radiation to be $T \sim 5K$. Remarkably, that CMB was first detected by accident, by Penzias and Wilson [16] in 1965, during radiometer calibrations that they used for satellite communication experiments at Bell Telephone Laboratories. This was a sensational discovery of radiation, that was emitted about thirteen and a half billion years ago, only a few hundred thousand years after the Big Bang, long before stars or galaxies ever formed. In 1978 they received the Nobel Prize in Physics for this discovery.

The formation of galaxies remained an open question. Already in 1946 Lifshitz [17] calculated that the amplitude of density perturbations grows

too slowly. To form galaxies, the right level of primordial density inhomogeneities was required: too small leads to the absence of galaxies, too large means having different structure than the observed one. Later, in 1967 Sachs and Wolfe [18] showed that the inhomogeneities may be potentially visible as small variations in the temperature of CMB in different directions on the sky. In 1992 the Cosmic Background Explorer (COBE) satellite confirmed this prediction with the detection of the CMB background radiation [19, 20] with an average temperature of $T \sim 2.7K$ and temperature variations of order 10^{-5}, that reflect the presence of small density inhomogeneities required for structure formation.

Despite the stunning successes of the hot Big Bang theory, supported by measurements of the CMB and observations of Hubble's Law together with predictions for the relative abundances of light elements during BBN [21–23], several problems remained unsolved. The first one is the *horizon problem*. Within the Big Bang cosmology, distinct patches of the CMB were not in causal contact at recombination. However, the observations show the isotropy in the CMB temperature across the entire sky and it is unclear why the causally-disconnected patches share similar physical properties. In addition to that, from the CMB data the geomety of the universe appears to be nearly flat. To satisfy within the Big Bang theory today's observed values, extremely flat initial conditions would be required. This fine-tuning forms the *flatness problem*. Finally, the *origin of primordial fluctuations* that seed all the structure remains unknown. In Section 1.2 we will show how the framework of cosmic inflation deals with the aforementioned problems.

1.2 Inflation

The main idea of the inflationary scenario is that the very early universe could be in an *unstable vacuum-like state* with high energy density and equation of state $p = -\rho$ that drives extremely rapid exponential expansion prior to the standard Big Bang evolution. After inflation ends, the vacuum energy is transformed into thermal energy in the form of the Standard Model particles, initiating the radiation dominated phase of the Universe. The transition from the phase of accelerated expansion to the thermal universe is called *reheating*, and will be described in detail in Sec. 1.3. Because of the exponential expansion, distant points on the CMB become causally connected and any initial curvature stretches to be nearly flat. That solves both the horizon and flatness problems. In addition to that, inflation also

explains the origin of structure in the universe, producing quantum density fluctuations that expanded during inflation, forming the higher density regions that condensed over the next several hundred million years into stars, galaxies and us.

Historically, the space that expands exponentially with a scale factor $a(t) \sim a_0\, e^{Ht}$, with H being the Hubble parameter, was first described in 1917 by de Sitter in [24, 25], even before Friedmann's solutions. However, for a long time its physical meaning remained unclear and it was used mostly for developing quantum field theory in curved space. The possibility of an exponential expansion during the early stages of the universe's evolution, although for superdense baryonic matter, was first considered by Gliner in [26]

In 1980 Guth [27] for the first time proposed a solution to the horizon and flatness problems by introducing the exponential expansion (inflation) of the universe trapped in a supercooled metastable vacuum state $\phi = 0$. Inflation was associated with the phase transition to a stable state $\phi_0 \neq 0$, and was accompanied by bubble nucleation via quantum tunneling. Bubble-wall collisions were responsible for reheating the universe, however collisions of the very large bubbles were destroying the homogeneity and isotropy after the end of inflation. This scenario was subsequently named as "old inflation".

The solution to this problem was introduced by Linde and independently by Albrecht and Steinhardt in [28, 29] and called the "new inflation" or "slow-roll inflation" scenario. In the new approach the supercooled state and tunneling out of a false vacuum state was not required any more, but instead inflation occurred when a scalar field ϕ was slowly rolling down its potential $V(\phi)$. The reheating era this time happens not because of bubble wall collisions, but via creation of elementary particles by damped oscillations of the classical field near the minimum of its potential.

1.2.1 Slow-roll inflation

The idea that inflation may be driven by a scalar field has revolutionized the whole cosmological community. Since inflationary dynamics is highly dependent on the underlying inflationary potential $V(\phi)$, a big variety of models have been already developed to date [1]. It is a challenge of the present-day cosmology to distinguish and falsify among all of them. Below we will describe the conditions on the potential that would enable inflation

[1] This may also be an effective description of some ultraviolet complete theory.

to happen.

Before we proceed, let us first outline the general conditions required for inflation to occur. To start with, the accelerated expansion $\ddot{a} > 0$ requires

$$\frac{\ddot{a}}{a} = H^2(1 - \epsilon_H) > 0, \tag{1.5}$$

where the parameter ϵ_H is called *the first Hubble slow-roll parameter* and defined as

$$\epsilon_H \equiv -\frac{\dot{H}}{H^2}. \tag{1.6}$$

The inequality (1.5) implies that to ensure the accelerated expansion, ϵ_H should be in the range $0 < \epsilon_H < 1$. In the limit $\epsilon_H \to 0$ the Hubble parameter $H = const$ and hence the space-time becomes de Sitter space $ds^2 = -dt^2 + e^{2Ht}dx^2$. In order for inflation to end, the space-time has to deviate from a perfect de Sitter space. However, for small and finite $\epsilon_H \ll 1$ de Sitter space remains a good approximation, that's why slow-roll inflation is often called a quasi-de Sitter period. To sum up, inflation requires $\epsilon_H < 1$, while the slow-roll inflation $\epsilon_H \ll 1$.

To solve the horizon and flatness problems, inflation has to last long enough. The current estimate is between 50 and 60 e-folds [2]. This condition is ensured by introducing *the second Hubble slow-roll parameter* [3]

$$\eta_H \equiv \frac{\dot{\epsilon}}{\epsilon H} \tag{1.7}$$

and the requirement $|\eta_H| \ll 1$. The above condition guarantees that the change of ϵ_H per Hubble time is small and therefore inflation can persist.

Finally, we can discuss what microscopic physics can lead to the conditions $\epsilon_H \ll 1$ and $|\eta_H| \ll 1$. We start from the general form of the action for the inflaton field $\phi(t, x)$ with a canonical kinetic term and a potential $V(\phi)$, minimally coupled to gravity, that is given by

$$S = \int d^4x\sqrt{-g}\left[\frac{M_{\rm pl}^2}{2}R - \frac{1}{2}\partial_\mu\phi\partial^\mu\phi - V(\phi)\right], \tag{1.8}$$

[2] Both problems are solved when the observable universe was smaller than the comoving Hubble radius at the beginning of inflation $(a_0H_0)^{-1} < (a_iH_i)^{-1}$. This restricts the number of e-folds of inflation to $N_{\rm tot} = \ln(a_e/a_i) > 64 + \ln(T_R/10^{15}{\rm Gev})$, with T_R being the reheating temperature. The number $N_{\rm tot}$ is smaller for the lower reheating temperature.

[3] Alternatively it may be defined as $\eta_H = -\frac{1}{2}\frac{\ddot{H}}{\dot{H}H}$.

where R is the Ricci scalar curvature of the space-time. The homogeneity and isotropy of the background implies the inflaton field depends only on time, i.e. $\phi = \phi(t)$. For the FLRW space-time its dynamics is governed by equations of motion

$$\ddot{\phi} + 3H\dot{\phi} + V_\phi = 0, \tag{1.9}$$

with $V_\phi = \frac{dV}{d\phi}$, together with two Friedmann equations

$$3M_{\rm pl}^2 H^2 = \frac{1}{2}\dot{\phi}^2 + V, \tag{1.10}$$

$$\dot{H} = -\frac{\dot{\phi}^2}{2M_{\rm pl}^2}. \tag{1.11}$$

With the above equations, the slow-roll parameters may be written in terms of the scalar field and its potential as

$$\epsilon_H = \frac{\frac{3}{2}\dot{\phi}^2}{\frac{1}{2}\dot{\phi}^2 + V}, \quad \eta_H = 2\frac{\ddot{\phi}}{H\dot{\phi}} + 2\epsilon_H. \tag{1.12}$$

To satisfy $\epsilon_H \ll 1$ and $|\eta_H| \ll 1$, one may see that the kinetic energy of the inflaton field has to be negligible in comparison to the potential one, as well as the field acceleration has to be small. This explains the name *slow-roll approximation*, which is defined as

$$\dot{\phi}^2 \ll V, \quad \ddot{\phi} \ll H\dot{\phi}. \tag{1.13}$$

The left inequality in (1.13) ensures that the Hubble parameter is nearly constant $\dot{H} \ll H^2$, leading to the quasi-exponential expansion with $a \sim e^{Ht}$. The right inequality allows one to neglect the acceleration term in (1.9) that assures long enough inflation. Slow-roll inflation is an attractor in the phase space $(\phi, \dot{\phi})$, which means that non-slow roll initial trajectories will very quickly converge to those that follow (1.13), as shown in Figure 1.1. For the review see for instance Ref. [30–32].

Comparing (1.10) - (1.11) with Friedmann equations (1.3) - (1.4), one may immediately find the energy density $\rho = \frac{1}{2}\dot{\phi}^2 + V(\phi)$ and pressure $p = \frac{1}{2}\dot{\phi}^2 - V(\phi)$ expressed in terms of the scalar field and its potential. In the slow-roll approximation this leads to the equation of state $w = p/\rho \approx -1$.

Alternatively, slow-roll conditions may be written in terms of the potential as

$$\epsilon_V \equiv \frac{M_{\rm pl}^2}{2}\left(\frac{\partial_\phi V}{V}\right)^2 \ll 1, \quad |\eta_V| \equiv M_{\rm pl}^2 \frac{|\partial_{\phi\phi}^2 V|}{V} \ll 1, \tag{1.14}$$

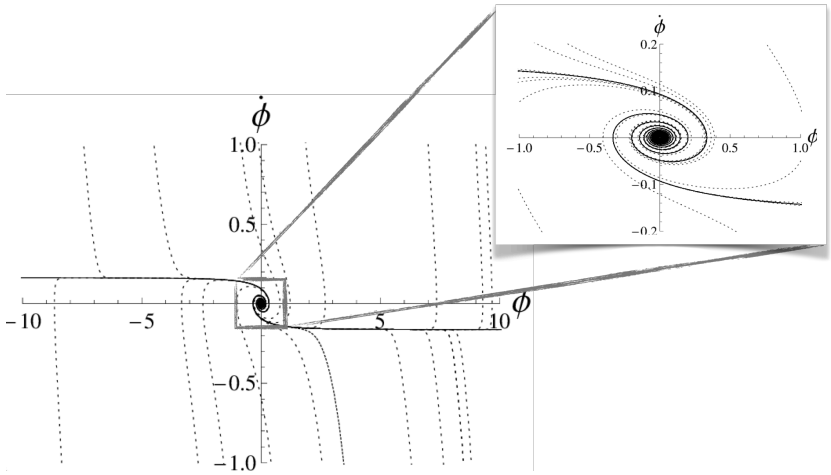

Figure 1.1: Attractor solutions for $m^2\phi^2$ potential with $m = 0.2M_{\rm pl}$ in $\phi - \dot\phi$ plane in units of $M_{\rm pl} = 1$. Solid curves are attractor solutions, that at large field values asymptote to $\dot\phi = \pm\sqrt{2/3}m$ and at small field values converge to the origin. Dotted curves show numerical solutions for random initial values. The top right plot is a zoom-in into the area around the origin. This figure is an adaptation of the one, presented in [31].

which are called *potential slow-roll parameters*. For single field models of inflation and in the slow-roll regime, the potential and the Hubble slow-roll parameters are related as

$$\epsilon_V \approx \epsilon_H, \quad \eta_V = 2\epsilon_H - \frac{1}{2}\eta_H. \tag{1.15}$$

However, in a broader class of models, including multi-field inflation, when the inflationary trajectory does not follow the gradient flow of the potential, their relation is much more involved, if possible at all [4].

1.2.2 Inflation beyond single-field approximation

Single field inflation is the leading framework for the early universe physics that sets the initial conditions and primordial density fluctuations in accordance with observations. However, the energy scale of the very early universe may be as high as 10^{15} GeV [5] and could contain multiple scalar fields that may participate in inflationary dynamics. Moreover, UV-complete theories typically lead to effective field theory descriptions with many distinct

[4] In multi-field inflation there is no good definition of η_V.

[5] The precise magnitude is unknown and this number should be taken as a reference value only.

fields, in flat as well as curved field-space geometries. This motivates the multi-field description of inflation, that we will outline below based on the covariant formalism described by van Tent et al in Refs. [33–37].

The general form of the action for multi-field inflation is given by

$$S = \int d^4x\sqrt{-g}\left[\frac{M_{\rm pl}^2}{2}R - \frac{1}{2}\mathcal{G}_{IJ}(\phi)g^{\mu\nu}\partial_\mu\phi^I\partial_\nu\phi^J - V(\phi)\right], \tag{1.16}$$

where $\mathcal{G}_{IJ}(\phi)$ is the field-space metric and $V(\phi)$ is a multi-field potential for scalar fields ϕ^I, with $I = 1\ldots n$, with n being the number of fields. The background solution $\phi_0^I(t)$ may be found from the following equations of motion

$$\mathcal{D}_t\dot{\phi}_0^I + 3H\dot{\phi}_0^I + \mathcal{G}^{IJ}V_{,J} = 0, \quad 3H^2 = \frac{1}{2}\dot{\phi}_0^2 + V, \tag{1.17}$$

where $\dot{\phi}_0 = \sqrt{\mathcal{G}_{IJ}\dot{\phi}_0^I\dot{\phi}_0^J}$ is the proper field velocity and $\mathcal{D}_t$ is a covariant derivative whose action on an arbitrary vector A^I is defined as $\mathcal{D}_tA^I \equiv \dot{A}^I + \Gamma^I_{JK}\dot{\phi}^JA^K$. Here Γ^I_{JK} are the Christoffel symbols associated with the metric $\mathcal{G}_{IJ}(\phi)$. In the multi-filed case the inflationary trajectory is a line in multi-dimensional space, non-geodesic in general. At each point along the trajectory unit vectors tangent and normal to the trajectory may be defined as

$$T^I \equiv \frac{\dot{\phi}^I}{\dot{\phi}_0}, \quad N_I \equiv -\frac{1}{|\mathcal{D}_tT|}\mathcal{D}_tT^I. \tag{1.18}$$

Next, the rate of turning (or simply, the angular velocity) of the inflationary trajectory is defined as

$$\Omega \equiv -N_I\mathcal{D}_tT^I. \tag{1.19}$$

The background equations of motion can be now projected into the tangent and normal directions and written in the following form

$$\ddot{\phi}_0 + 3H\dot{\phi}_0 + V_T = 0, \quad V_N = \dot{\phi}_0\Omega, \tag{1.20}$$

with $V_T = T^IV_I$ and $V_N = N^IV_I$, such that the gradient of the potential is written as $V_I = T_IV_T + N_IV_N$. For $\Omega = 0$ the field dynamics reduces to the single field description and the background motion is geodesic. In general, however, $\Omega \neq 0$, which may bring potentially observable physical signatures, such as features in the primordial power spectra [36], that can also lead to generation of primordial black holes and gravitational waves, see recent works on this topic [38–40] and references therein.

Non-zero turn rate also distinguishes the potential and Hubble slow roll parameters in the multi-field case. The potential first slow-roll parameter in the multiple-field case may be defined as [41]

$$\epsilon_V \equiv \frac{1}{2}\frac{V^I V_I}{V^2}. \tag{1.21}$$

It follows [41, 42] that two alternative definitions of first slow-roll parameters in multi-field inflation now are related as

$$\epsilon_V = \epsilon_H \left(1 + \frac{\Omega^2}{9H^2}\right), \tag{1.22}$$

which clearly shows how different ϵ_V and ϵ_H are in case of a non-zero turn rate.

1.2.2.1 Muti-field inflation vs Swampland conjectures

The discussion regarding ultraviolet (UV) complete theories may lead to the absolutely legitimate question: can inflation be embedded into a full quantum theory of gravity? There are two ways to talk about this problem. The first one is the so-called *top-down approach*, which takes some UV complete theory, like string M- or F-theory in higher dimensional space and via compactification to four-dimensional space-time conclude which common features do the effective field theories (EFT) share. The second way is to follow *the bottom-up approach*, the essence of which is to start with a four-dimensional EFT coupled to gravity and identify the consistency criteria that quantum gravity sets. Recently, Vafa in [43] introduced consistency criteria named *swampland conjectures*. Before this work there were other studies in this direction, however they have not gained so much attention. For the recent reviews on the subject see Refs. [44–47]. The swampland represents the space of quantum field theories which are incompatible with quantum gravity, opposite to the landscape, which includes compatible EFTs with possible UV completions. The two conjectures directly question the possibility of a UV embedding for single-field inflation [48]. We will briefly discuss them below [6], taking into account also the recent investigations mentioned above.

Two necessary conditions that low energy four dimensional EFT, obtained from string theory compactifications, conjectured to satisfy are:

[6] This is an active research direction nowadays and we present here the state of the art of 2021.

- *Swampland distance conjecture.* Quantum gravity effects sets a maximum distance in field space beyond which the low energy description is not valid any more
$$\Delta\phi < M_{\rm pl}\Delta, \tag{1.23}$$
where $\Delta \sim \mathcal{O}(1)$.

- *Swampland de Sitter conjecture.* The potential of the four-dimensional EFT should be steep enough to satisfy
$$M_{\rm pl}\frac{|\nabla V|}{V} \geqslant c \quad \text{or} \quad \min(\nabla_i\nabla_j V) \leqslant \frac{-c'V}{M_{\rm pl}^2} \tag{1.24}$$
where $c, c' \sim \mathcal{O}(1)$.

While the swampland distance conjecture is in a mild tension with single-field inflation, the de Sitter conjecture has far more dramatic implications. As we have seen in Sec. 1.2.1, the first slow-roll parameters should satisfy $\epsilon_H \simeq \epsilon_V \ll 1$, which automatically constrains the inflationary potential to be flat, in order for slow-roll inflation to happen. This is in tension with the requirement (1.24) and satisfying simultaneously $\Delta \sim \mathcal{O}(1)$, $c, c' \sim \mathcal{O}(1)$. Hence, if the criteria are true, this questions the existence of flat directions in the potential or de Sitter minima, and therefore all single field inflation models.

However, this is not the case for multi-field inflation. As was shown in [41], when the inflationary trajectory is non-geodesic and has a non-zero turning rate, it is possible to simultaneously satisfy both aforementioned swampland conjectures. Because of the relation (1.22), it is possible to have successful inflation with both $\epsilon_H \ll 1$ and $\epsilon_V \sim \mathcal{O}(1)$ when $\Omega^2/H^2 \gg 1$. In addition to that, there is a lower bound on the turning rate Ω to satisfy the second conjecture and agree with CMB observations.

It is worth mentioning, that the rigorousness of swampland conjectures is still debated in the scientific community. Despite this, it is an important step towards a better understanding of the UV completion of inflationary cosmology and EFTs in general.

1.2.2.2 Inflation in curved field-space

Besides discussions about the shape of the inflationary potential $V(\phi)$, for multi-field inflation there is also a freedom in the choice of the field-space metric $\mathcal{G}_{IJ}(\phi)$ that is defined in the action (1.16).

A revival of interest in curved field-space geometries was initiated by Kallosh and Linde, with the development of their inflationary *α-attractor model* [49–52]. Following the top-down approach discussed in the previous section, this class of models originate from supergravity theories with a special choice of the Kähler potential and superpotential. The hyperbolic geometry, that is inherited by the theory, provides the exponential stretching for the inflationary potentials, creating flat plateaus ideal for slow-roll inflation. Because any initial potential is stretched exponentially, the α-attractor model provides universal predictions for the scalar spectral index and tensor-to-scalar ratio, that so far are in the very good agreement with the latest observational constraints [53]. It is remarkable that, because of the UV nature, this model is intrinsically a multi-field model of inflation. In Chapter 4 we will present a comprehensive analysis of the reheating process for the two-field α-attractors and demonstrate the significance of the curved field-space geometry for efficient transition to the radiation-dominated state of the universe.

A number of research works has followed after the appearance of α-attractors. In particular, it was shown that the negative curvature of the field space manifold may lead to tachyonic instabilities that destabilize inflationary trajectories. This phenomenon was called *the geometrical destabilization* of inflation [54–58]. Such instability may be catastrophic for inflation, since huge instabilities may terminate it too early, however is beneficial for reheating as will be discussed in more detail in the Part II of the thesis. Another possible evolution scenario with a non-trivial field-space manifold where the inflaton field orbits to the bottom of its potential, was introduced in [59] and called *hyperinflation*. It has drawn a lot of attention and was followed by various developments in the context of non-trivial field-space geometries and multi-field inflation [60–68].

One particular class of multi-field inflationary models was developed in [69–73] and is called *the ultra-light isocurvature scenario*. In these models, the perturbations orthogonal to the inflationary trajectory are massless, but efficiently coupled to the inflaton. They freeze on superhorizon scales and source the tangential (curvature) perturbation, that results in the primordial observables at the end of inflation having a similar phenomenology as in the single-field case. The first exact realization of the ultra-light isocurvature scenario is called *shift-symmetric orbital inflation* and will be discussed in Chapter 2.

1.2.3 Gauge fields during inflation

Gauge fields are unavoidable ingredients of any realistic field theory. For instance, in the Standard Model the strong, electromagnetic, and weak interactions are described by a non-Abelian gauge theory with the symmetry group $U(1)\times SU(2)\times SU(3)$, with the total amount of twelve gauge bosons that include the photon, three weak boson and eight gluons.

Typically, scalar fields are the main characters of inflationary frameworks, however gauge fields can also drive isotropic inflation [7]. In [74, 75] it was shown that gauge fields minimally coupled to gravity with a Lagrangian of the form

$$\mathcal{L}=\mathcal{L}\left(g_{\mu\nu},F_{\mu\nu}\right)=\frac{M_{\rm Pl}^2}{2}R+\mathcal{L}_G\left(F_{\mu\nu}\right), \tag{1.25}$$

may lead to inflationary solutions. Here $F^A_{\mu\nu}=\partial_\mu A^A_\nu-\partial_\nu A^A_\mu-gf^{ABC}A^B_\mu A^C_\nu$ is the field strength of the gauge field, g is the gauge coupling and f^{ABC} are structure constants with gauge indices $A=1,2,\ldots,dimG$ of the gauge group G. The generators are denoted as T^A with the standard normalization $[T^A,T^B]=if^{ABC}T^C$ and $Tr(T^AT^B)=\frac{1}{2}\delta^{AB}$. Above $\mathcal{L}_G\left(F_{\mu\nu}\right)$ is a general diffeomorphism- and gauge-invariant Lagrangian that may contain powers of $F_{\mu\nu}$, where the space-time indices are summed up via the metric $g_{\mu\nu}$ or the Levi-Civita tensor $\epsilon^{\mu\nu\rho\sigma}$, and gauge indices are summed by taking the trace. The change under the local gauge transformation with $U\in G$ is defined as

$$A_\mu \quad\longrightarrow\quad A'_\mu=-\frac{i}{g}U^{-1}\partial_\mu U+U^{-1}A_\mu U, \tag{1.26}$$

$$F_{\mu\nu} \quad\longrightarrow\quad F'_{\mu\nu}=U^{-1}F_{\mu\nu}U. \tag{1.27}$$

In this set-up the choice of the non-Abelian gauge group is crucial. In the Abelian case, in order to preserve the rotational symmetry of the flat FLRW background, only the time-component of a vector gauge field may be non-zero and depend solely on time due to homogeneity. Hoverer, such a choice leads to a pure gauge configuration, since it implies the vanishing field strength of the gauge field. By contrast, the choice of non-Abelian gauge group allows us to keep spatial components A_i non-zero and at the same time preserve rotational symmetry. To understand this, first let us note that the time component A_0 may be always set to zero by fixing a gauge to a temporal gauge, i.e. there is always $U=U(t)$ such that $A'_\mu=0$.

[7] This section in mainly based on [76].

This fixes the gauge freedom up to space-time independent global gauge transformations. The remaining global gauge transformations may be used to preserve the rotational invariance, since due to gauge transformations (1.26) two fields are related as $(A_i)_G = U^{-1}A_\mu U \equiv_G A_i$, with constant $U \in G$. It is known that upon spatial rotations $A \to (A_i)_R = R_{ij}A_j$. Hence, the rotational symmetry is preserved if the background configuration is chosen such that $A_R = A_G$. Since any non-Abelian gauge group has an $SU(2)$ subgroup, the gauge group G may be chosen to be $SU(2)$ or $SO(3)$ without loss of generality.

To sum up, a rotationally invariant and homogeneous background is achieved via the ansatz

$$A^a_0 = 0, \tag{1.28}$$

$$A^a_i = \delta^a_i a(t)Q(t), \tag{1.29}$$

where $a(t)$ is a scale factor and $Q(t)$ is a vacuum expectation value (VEV) of the gauge field. In this ansatz the gauge group G is chosen to be $SU(2)$ and, hence, $A \equiv a = 1, 2, 3$.

Now let us come back to (1.25) and see that together with (1.28),(1.29) it may indeed lead to inflationary solutions, i.e. to achieve simultaneously $\rho + 3p < 0$ and $\rho > 0$. The simplest possible choice for $\mathcal{L}_G(F_{\mu\nu})$ would be the Yang-Mills lagrangian, i.e. $\mathcal{L}_G(F_{\mu\nu}) = -\frac{1}{4}F^a_{\mu\nu}F^{a\,\mu\nu}$. However, in the Yang-Mills theory $\rho + 3p = 2\rho > 0$, which have the equation of state of radiation. Another choice is to consider higher terms in $F^a_{\mu\nu}F^{b\mu\nu}$, but the conditions to obtain accelerated expansion are not easily satisfied there [77–84]. The way out is to involve terms with $\epsilon^{\mu\nu\rho\sigma}$. The first possibility would be $F \wedge F \propto \epsilon^{\mu\nu\rho\sigma}F^a_{\mu\nu}F^a_{\rho\sigma}$, which is a total derivative and does not contribute to the energy momentum tensor. Hence, the simplest non-trivial choice appears to be $(F \wedge F)^2 = \frac{1}{4}(\epsilon^{\mu\nu\rho\sigma}F^a_{\mu\nu}F^a_{\rho\sigma})^2$, which leads to $p = -\rho$ and hence satisfies the desired criteria.

Taking into account the aforementioned arguments, Refs. [74, 75] proposed the Gauge-flation action of the form

$$S = \int d^4x\sqrt{-\det(g_{\mu\nu})}\left[\frac{M^2_{\rm Pl}}{2}R - \frac{1}{4}F^a_{\mu\nu}F^{a\,\mu\nu} + \frac{\kappa}{384}\left(\epsilon^{\mu\nu\rho\sigma}F^a_{\mu\nu}F^a_{\rho\sigma}\right)^2\right], \tag{1.30}$$

where $\kappa > 0$ is a parameter of the theory with dimension $M^{-4}_{\rm pl}$. The energy-momentum tensor is given by

$$T_{\mu\nu} \equiv \frac{-2}{\sqrt{-\det(g_{\mu\nu})}}\frac{\delta\left(\sqrt{-\det(g_{\mu\nu})}\mathcal{L}\right)}{\delta g^{\mu\nu}} = 2\frac{\delta\mathcal{L}}{\delta F^a{}_{\sigma}{}^{\mu}}F^a{}_{\sigma\nu} + g_{\mu\nu}\mathcal{L}, \tag{1.31}$$

which for a homogeneous and isotropic configuration takes the form of the energy-momentum tensor of a perfect fluid. From the above action it follows that

$$\rho = \rho_{\rm YM} + \rho_\kappa, \quad p = \frac{1}{3}\rho_{\rm YM} - \rho_\kappa, \tag{1.32}$$

where $\rho_{\rm YM}$ stands for the energy density contribution from the Yang-Mills part of the action and ρ_κ from the $(F \wedge F)^2$. When $\rho_\kappa \gg \rho_{\rm YM}$, the equation of state $w \approx -1$ which indicates the desired phase of accelerated expansion.

In [74–76, 85] it was shown that the action (1.30) indeed leads to an attractor solution and the isotropic background is stable with regard to the initial anisotropies and choice of initial conditions.

Despite of the beautiful idea of incorporating gauge fields as inflatons, the Gauge-flation model does not match the observational constraints. It turns out that it is impossible to satisfy simultaneously the bounds for the tensor-to-scalar ratio and scalar spectral tilt. However, the search for alternative gravitational wave production mechanisms initiated renewal of interest in models that involve gauge fields. These, based on [86], will be discussed in more detail in Chapter 3.

1.2.4 Observations

To extract observables from the inflationary epoch, in 1980-1990s Bardeen, Kodama, Sasaki, Mukhanov et al [87–91] developed *the cosmological perturbation theory*. We will briefly outline how quantum perturbations that originate during inflation generate the temperature anisotropies in the CMB as well as produce gravitational waves.

1.2.4.1 Perturbation theory

The small perturbations of the metric and the energy-momentum tensor may be written as [8]

$$\begin{aligned} g_{\mu\nu}(t,x) &= \bar{g}_{\mu\nu}(t) + \delta g_{\mu\nu}(t,x), \\ T_{\mu\nu}(t,x) &= \bar{T}_{\mu\nu}(t) + \delta T_{\mu\nu}(t,x), \end{aligned} \tag{1.33}$$

where $\bar{g}_{\mu\nu}$ is the background flat FLRW metric (1.1) and $\bar{T}_{\mu\nu}(t)$ the homogeneous and isotropic energy-momentum tensor. Here $\mu = 0, 1, 2, 3$ denote the space-time indices. It is convenient to perform a scalar-vector-tensor

[8] This Section is based mainly on [4].

(SVT) decomposition of the perturbations, then the perturbed space-time metric takes the form

$$ds^2 = -(1+2A)dt^2 - 2a(t)B_i dx^i dt + a^2(t)(\delta_{ij}+h_{ij})dx^i dx^j, \qquad (1.34)$$

where $i,j = 1,2,3$ label the spatial directions. Here the 3-vector B_i may be written as a combination of the gradient of a scalar and a divergenceless vector $B_i = \partial_i B + \hat{B}_i$ with $\partial^i \hat{B}_i = 0$, and the rank-2 symmetric tensor h_{ij} may de decomposed into a scalar, vector and tensor as $h_{ij} = 2C\delta_{ij} + 2\partial_{\langle i}\partial_{j\rangle}E + 2\partial_{(i}\hat{E}_{j)} + \hat{E}_{ij}$ with divergenceless vector $\hat{E}_i$ that satisfy $\partial^i \hat{E}_i = 0$ and a divergenceless and traceless tensor perturbation $\hat{E}_{ij}$ with $\partial^i \hat{E}_{ij} = 0$, $\hat{E}^i_i = 0$ and

$$\begin{aligned} \partial_{\langle i}\partial_{j\rangle}E &\equiv \left(\partial_i\partial_j - \frac{1}{3}\delta_{ij}\nabla^2\right)E, \\ \partial_{(i}\hat{E}_{j)} &\equiv \frac{1}{2}\left(\partial_i\hat{E}_j + \partial_j\hat{E}_i\right). \end{aligned} \qquad (1.35)$$

Hence, perturbations decompose into scalars: A, B, C, E; vectors: $\hat{B}_i, \hat{E}_i$; tensors: $\hat{E}_{ij}$, which have 4+4+2 degrees of freedom (d.o.f.) respectively. Invariance of the theory under the coordinate transformations removes 4 more d.o.f., leading to only 6 physical d.o.f. At linear order the Einstein equations for scalars, vectors and tensors do not mix and hence can be studied separately. This is why the SVT decomposition is useful. Vector perturbations quickly decay with the expansion of the universe and not produced at all in standard single-field inflationary models. Therefore, we will focus only on the description of scalar and tensor perturbations in the forthcoming sections.

Before we proceed further, let us note that the metric perturbations in (1.34) depend on the choice of coordinate system, i.e. are gauge dependent, and hence are not uniquely defined. This problem was resolved by Bardeen [87], who introduced special combinations of metric perturbations that do not change under coordinate transformations. Gauge invariant variables are called *the Bardeen variables* and defined as

$$\begin{aligned} \Psi &\equiv A + \mathcal{H}(B - E') + (B - E')', \qquad & \hat{\Phi}_i &\equiv \hat{B}_i - \hat{E}_i', \\ \Phi &\equiv -C + \frac{1}{3}\nabla^2 E - \mathcal{H}(B - E'), & \hat{E}_{ij}&, \end{aligned} \qquad (1.36)$$

which for convenience are written in conformal time $d\tau \equiv dt/a(t)$ with the conformal Hubble rate $\mathcal{H} = a'/a$. These variables cannot be removed by a

gauge transformation. Two more gauge-invariant quantities that combine metric and matter perturbations are called *curvature perturbations*

$$\begin{aligned}\zeta &= -C + \frac{1}{3}\nabla^2 E + \mathcal{H}\frac{\delta\rho}{\bar{\rho}'},\\ \mathcal{R} &= -C + \frac{1}{3}\nabla^2 E - \mathcal{H}(v+B),\end{aligned} \tag{1.37}$$

where $v_i = \partial_i v$ is the bulk velocity, that appears from the perturbed energy-momentum tensor, in particular $T^i{}_0 = (\bar{\rho}+\bar{p})v_i$. In case of the adiabatic fluctuations, ζ and $\mathcal{R}$ become constant and coincide with each other on the scales where the physical wavelength is larger than the comoving horizon. As we will see in the next section, they play a major role in describing scalar perturbations from inflation.

Another possibility to deal with the gauge-dependence is to fix the gauge, i.e. set two of the four scalar metric perturbations to zero: $B = E = 0$ in *the Newtonian gauge*, $C = E = 0$ in *the spatially-flat gauge* and $A = B = 0$ in *synchronous gauge*.

1.2.4.2 Scalar perturbations in single field-inflation

Let us start by describing [9] the scalar fluctuations for the single field inflationary action (1.8) by perturbing the matter inflaton field as

$$\phi(t,x) = \bar{\phi}(t) + \delta\phi(t,x), \tag{1.38}$$

where $\bar{\phi}(t)$ is a solution to the background equations of motion. The coupling of the inflaton perturbations $\delta\phi$ to the metric depends on the gauge choice. We fix the gauge to the spatially flat one, meaning that A and B are related to the inflaton fluctuations through the Einstein equations. Solving the Einstein equations together with the equations of motion of the perturbed field, leads to the linear equation of motion for the gauge-invariant perturbations. Introducing variables $f \equiv a\,\delta\phi$ and $z \equiv \frac{a\bar{\phi}'}{\mathcal{H}}$ and going to Fourier space results in *the Mukhanov-Sasaki equation* for the mode functions

$$f_k'' + \left(k^2 - \frac{z''}{z}\right) f_k = 0. \tag{1.39}$$

This is the master equation for inflationary perturbations. It is valid on all scales, exact (does not assume the slow-roll approximation) and contains the coupling between matter and metric fluctuations. This equation has the

[9] More detailed analysis may be found for instance in Refs. [3, 4, 92].

form of the harmonic oscillator equation with a time-dependent frequency $\omega^2(k,\tau) = k^2 - \frac{z''}{z}$. With the knowledge of the second order action for the Fourier components of the inflaton perturbations, the quantization of the theory is performed in complete analogy with the quantum harmonic oscillator problem. The quantisation of the field f is implemented as

$$\hat{f}(\tau,x) = \frac{1}{(2\pi)^3}\int d^3k \left[f_k(\tau)\hat{a}_k(t)e^{-i\mathbf{kx}} + f_k(\tau)^*\hat{a}_k^\dagger e^{i\mathbf{kx}}\right], \tag{1.40}$$

where $\hat{a}_k^\dagger, \hat{a}_k$ are creation and annihilation operators that satisfy the canonical commutation relations.

Next we can get back to the analysis of solutions of the Mukhanov-Sasaki equation. For $k \gg |z''/z|$, the frequency is constant and proportional to the wave number k, which leads to the oscillating solutions that match *the Bunch-Davies vacuum* in the asymptotic past $\lim_{\tau\to-\infty} f_k = \frac{e^{-ik\tau}}{\sqrt{2k}}$. Since $\frac{z''}{z} \approx 2\mathcal{H}^2$ during slow-roll, it is a measure of the comoving horizon $\mathcal{H}^{-1}$. Therefore, the regime above corresponds to $k \gg \mathcal{H}$, which denotes *the sub-Hubble* scales. With time the comoving Hubble scale shrinks, and modes at some moment in time cross and exit it. The relation $k \ll \mathcal{H}$ distinguishes *the super-Hubble* scales, on which the frequency $\omega(k,\tau)$ becomes imaginary. In this regime there is a growing $f_k \propto z$ and a decaying solution $f_k \propto z^{-2}$ for perturbation modes. The growing solution is the relevant one for observations [10]. It implies that the gauge-invariant curvature perturbation defined in (1.37) is conserved on super-Hubble scales, specifically

$$\mathcal{R}_k = -\frac{\mathcal{H}}{\bar{\phi}'}\delta\phi_k = -\frac{f_k}{z} = const. \tag{1.41}$$

In particular, in the slow-roll approximation the solution of (1.39) is given by

$$f_k(\tau) = \frac{\sqrt{\pi}}{2}\sqrt{-\tau}H_\nu^{(1)}(-k\tau), \quad \text{with} \quad \nu \equiv \frac{3}{2} + \epsilon_H + \frac{1}{2}\eta_H. \tag{1.42}$$

where $H_\nu^{(1)}$ is the Hankel function of the first kind.

The next step is to find the quantum statistics for the operator $\hat{f}$. The expectation value of it is zero $\langle 0|\hat{f}|0\rangle = 0$, but the variance is not and is given by

$$\langle|\hat{f}|^2\rangle \equiv \langle|\hat{f}(\tau,0)\hat{f}(\tau,0)|0\rangle = \int d\ln k \frac{k^3}{2\pi^2}|f_k(\tau)|^2. \tag{1.43}$$

[10] Decaying mode can be relevant in some multi-field set-ups.

The dimensionless power spectra for mode functions is defined as

$$\Delta_f^2(k,\tau) \equiv \frac{k^3}{2\pi^2}|f_k(\tau)|^2, \tag{1.44}$$

which leads to the power spectra for $\delta\phi$ fluctuations

$$\Delta_{\delta\phi}^2(k,\tau) = \frac{\Delta_f^2(k,\tau)}{a^2(\tau)} \approx \left(\frac{H(t)}{2\pi}\right)^2\Bigg|_{k=aH}. \tag{1.45}$$

Finally, we have all the necessary ingredients to relate the fluctuations in the inflaton field to observable fluctuations after inflation. Since the curvature perturbation freezes on super-Hubble scales, it is a perfect quantity to provide this link. The dimensionless power spectrum $\Delta_{\mathcal{R}}^2(k)$ is defined by

$$\langle \mathcal{R}_k \mathcal{R}_{k'}\rangle = (2\pi)^3\delta^{(3)}(k+k')P_{\mathcal{R}}(k), \quad \Delta_{\mathcal{R}}^2(k) = \frac{k^3}{2\pi^2}P_{\mathcal{R}}(k). \tag{1.46}$$

Therefore, the power spectrum of $\mathcal{R}$ can be computed via the power spectrum of $\delta\phi$, evaluated at the horizon crossing $k = aH$, which results into

$$\Delta_{\mathcal{R}}^2(k) = \left(\frac{H}{\dot{\phi}}\right)^2 \Delta_{\delta\phi}^2 = \frac{1}{8\pi^2\epsilon_H}\frac{H^2}{M_{\rm pl}^2}\Bigg|_{k=aH}. \tag{1.47}$$

Even though during the slow-roll inflation both $\epsilon_H(t)$ and $H(t)$ depend on time very mildly, they have different values when different modes cross the horizon. This introduces a source of scale dependence, which is captured by the parameter named as *the scalar spectral index* and defined as

$$n_s - 1 \equiv \frac{d\ln\Delta_{\mathcal{R}}^2(k)}{d\ln k}, \quad \Delta_{\mathcal{R}}^2(k) = A_s(k_*)\left(\frac{k}{k_*}\right)^{n_s-1}, \tag{1.48}$$

where $A_s(k_*)$ is the amplitude of the scalar power spectrum at *the pivot scale* k_*, at which the reference scale exit the horizon. The scalar spectral index may be written in terms of the slow-roll parameters as

$$n_s = 1 - 2\epsilon_H - \eta_H. \tag{1.49}$$

Currently the observations show deviation from scale-invariance at 5.6σ confidence level [53] with values $n_s = 0.9603 \pm 0.0073$ for $k_* = 0.05\text{Mpc}^{-1}$, which is a direct measurement of time dependence during the inflationary dynamics [11].

[11] Assuming inflation is the right explanation.

The higher order correlation functions reflect non-Gaussian initial conditions (IC's) that are associated with *primordial non-Gaussianity*. Here IC's refer to those created by inflation, that will be subsequently stretched to macroscopic scales, become classical and provide seeds for the cosmic structure. Within linear perturbation theory, an initial Gaussian probability distribution will not change throughout the evolution, meaning that the amplitude of perturbations will have Gaussian shape around the mean value. Higher order correlations then test the deviations from the Gaussian distribution of the IC's of perturbations. Whereas the two-point correlation function probes a free theory, the three-point function is associated with non-linear interactions and hence encodes the particle content and the interactions during inflation. The primordial bispectrum is the Fourier transform of the three-point correlation function of curvature perturbation, defined as

$$\langle \mathcal{R}_{k_1} \mathcal{R}_{k_2} \mathcal{R}_{k_3} \rangle = (2\pi)^3 \delta^{(3)}(k_1 + k_2 + k_3) \frac{(2\pi^2)^2}{(k_1 k_2 k_3)^2} B_{\mathcal{R}}(k_1, k_2, k_3). \quad (1.50)$$

Because of the homogeneity of the background, the momentum three-vectors add up to zero and hence form a triangle. Depending on the shape of this triangle, the signal will also change. Typically, the most commonly studied are equilateral, local and folded shapes. The amplitude of the non-Gaussianity is defined in equilateral configuration ($k_1 = k_2 = k_3$) as

$$f_{\rm NL}(k) \equiv \frac{5}{18} \frac{B_{\mathcal{R}}(k, k, k)}{\Delta^4_{\mathcal{R}}(k)}, \quad (1.51)$$

which allows one to express the bispectrum as

$$B_{\mathcal{R}}(k_1, k_2, k_3) \equiv \frac{18}{5} f_{\rm NL} \times S(x_2, x_3) \times \Delta^4_{\mathcal{R}}(k), \quad (1.52)$$

where $x_2 \equiv k_2/k_1$, $x_3 \equiv k_3/k_1$ and $S(x_2, x_3)$ is the shape function. The current constraint from CMB observations on the amplitude of local non-Gaussianity is $f^{\rm local}_{\rm NL} = -0.9 \pm 5.1$.

1.2.4.3 Scalar perturbations with multiple fields

Similarly as in the single-field case, the perturbations $\delta\phi^I(x^\mu)$ to the background field trajectories $\varphi^I(t) \equiv \phi^I_0(t)$ may be written as

$$\phi^I(x^\mu) = \varphi^I(t) + \delta\phi^I(x^\mu), \quad (1.53)$$

where I runs through the number of fields in the underlying theory. The perturbations may be combined into the gauge-invariant Mukhanov-Sasaki variable [88, 91, 93, 94]

$$Q^I \equiv \delta\phi^I + \frac{\dot{\phi}^I}{H}\psi. \tag{1.54}$$

Then, from the background equations of motion (1.17), one finds the equation of motion for perturbations Q^I in the form

$$\mathcal{D}_t^2 Q^I + 3H\mathcal{D}_t Q^I + \left[\frac{k^2}{a^2}\delta^I{}_J + \mathcal{M}^I{}_J\right] Q^J = 0, \tag{1.55}$$

with the mass-squared matrix defined by

$$\mathcal{M}^I{}_J \equiv \mathcal{G}^{IK}\left(\mathcal{D}_J\mathcal{D}_K V\right) - \mathcal{R}^I{}_{LMJ}\dot{\varphi}^L\dot{\varphi}^M - \frac{1}{M_{\rm pl}^2 a^3}\mathcal{D}_t\left(\frac{a^3}{H}\dot{\varphi}^I\dot{\varphi}_J\right). \tag{1.56}$$

Here the first term is the analogue of the Hessian of the potential, calculated in a curved field space defined by the field metric $\mathcal{G}^{IJ}(\varphi^K)$. The second contribution resembles the right-hand side of the geodesic deviation equation, where $\mathcal{R}^I{}_{LMJ}$ is the Riemann tensor calculated from the field-space metric $\mathcal{G}_{IJ}(\varphi^K)$. Hence it indicates how two distinct trajectories in field space approach or recede from each other. This term is a unique consequence of the non-trivial field geometry and is identically zero in single-field models or models with canonical kinetic terms. Finally, the third term encodes the kinematic effects, such as turns in the field trajectory.

In the case with multiple fields it is convenient to classify the scalar perturbations in two types: the adiabatic (curvature) perturbations that are tangential to the inflationary trajectory and the isocurvature perturbations, that are orthogonal to it. Let us focus on the case with two fields and project the perturbations along the tangent T^I and normal directions N^I, defined in Section 1.2.2. Then the second order action for curvature $\mathcal{R}$ and isocurvature σ perturbations is given by [69]

$$S_2 = \int d^4x a^3 \left[\epsilon_H\left(\dot{\mathcal{R}} - \frac{2\Omega}{\sqrt{2\epsilon_H}}\sigma\right)^2 - \frac{\epsilon_H}{a^2}(\partial_i\mathcal{R})^2 + \frac{1}{2}\left(\dot{\sigma}^2 - \frac{1}{a^2}(\partial_i\sigma)^2\right) - \frac{1}{2}\mu^2\sigma^2\right], \tag{1.57}$$

where Ω is the turning rate of the trajectory defined in (1.19) and μ is the mass of the isocurvature mode that can be written as

$$\mu^2 = V_{NN} + \epsilon_H\mathbb{R}H^2 + 3\Omega^2. \tag{1.58}$$

Here $V_{NN} = N^I N^J \nabla_I \nabla_J V$ is the analogue of the Hessian of the potential and $\mathbb{R}$ is the Ricci scalar computed from the field-space metric $\mathcal{G}_{IJ}$. From (1.57) one can see that if the turn rate Ω is non-zero, the curvature and isocurvature perturbations get coupled. This is an important property of multi-field inflationary models. Depending on the magnitude of μ with regard to the Hubble scale H, multi-field models may be divided into three different cases. The case when $\mu \gg H$ corresponds to the regime with heavy fields. They may be integrated out that leads to the effective single-field theory with a reduced sound speed [36, 95–98]. Another regime with $\mu \sim \mathcal{O}(H)$ corresponds to the quasi-single field regime and was studied in [99–101]. The regime $\mu \ll H$ corresponds to the case with light isocurvature fields, that was extensively studied within the curvaton scenario [102, 103].

The case with $\mu^2 = 0$, however, is special. In this case the above action is invariant under the shift of both $\dot{\mathcal{R}}$ and σ. This ensures that σ behaves as a massless perturbation on super-Hubble scales and acts as a constant source for the curvature perturbation. Such situation will be discussed in detail in Chapter 2 of the thesis. We will also get back to the general discussion of multi-field perturbations in Part II of the thesis in Section 1.3.3, with further focus on the reheating era.

1.2.4.4 Tensor modes

After 100 years from the discovery of Einstein's General Relativity theory, the LIGO/VIRGO collaboration [104–109] announced the direct observation of gravitational waves (GW), which opened the era of GW astronomy. In addition to astronomical observations, GW interferometers allow us to directly probe the physics of the early Universe via the stochastic gravitational wave background (SGWB). The latter differs considerably from the gravitational waves coming from binary inspirals and burst events or continuous periodic gravitational waves that originate from pulsars. The signal from such events is coming from a specific direction, whereas the SGWB, similarly to the CMB, is uniform in all directions. Remarkably, its potential observation (as well as the absence of this observation) would give unique information about the physics of the early Universe, in particular the energy scale of inflation which is encoded in the Hubble parameter.

The GWs originate from tensor perturbations of the FRW metric (1.34)

$$ds^2 = -dt^2 + a(t)^2 \left(\delta_{ij} + h_{ij}\right) dx^i dx^j, \tag{1.59}$$

where the perturbation h_{ij} is symmetric, trace-free and transverse.

From the perturbed Einstein equations

$$\bar{G}_{\mu\nu} + \delta G_{\mu\nu} = 8\pi G \left(\bar{T}_{\mu\nu} + \delta T_{\mu\nu}\right), \tag{1.60}$$

it follows that the equation of motion for tensor perturbation in Fourier space appears in the form (see for instance [110, 111])

$$\ddot{h}_{ij} + 3H\dot{h}_{ij} + k^2 h_{ij} = 16\pi G \Pi_{ij}^{TT}, \tag{1.61}$$

where Π_{ij}^{TT} is the transverse-traceless part of the anisotropic stress tensor. In standard slow-roll single field inflationary models the anisotropic stress tensor is identically zero and amplification of the tensor vacuum metric fluctuations occurs because of the exponential expansion during inflation. It is convenient to align the z-axis with the momentum of the mode $\vec{k} = (0, 0, k)$ and write h_{ij} in terms of the two polarization modes of the gravitational wave

$$\frac{M_{\rm pl}}{2} a h_{ij} \equiv \frac{1}{\sqrt{2}} \begin{pmatrix} f_+ & f_\times & 0 \\ f_\times & -f_+ & 0 \\ 0 & 0 & 0 \end{pmatrix}. \tag{1.62}$$

Such parametrization reduces the equation of motion (1.61) to two copies of the equation of motion (1.39) with $\frac{z''}{z} = \frac{a''}{a}$ for massless scalar fields f_+ and $f_\times$. Hence, for each mode $f_+, f_\times$ the computation is performed exactly in the same way as for the case of scalar perturbations. The tensor power spectrum is then simply a rescaling of (1.45) by a factor $2 \times \left(\frac{2}{M_{\rm pl}}\right)^2$ that accounts for the sum of two polarizations and the normalization in (1.62) respectively. Hence, the tensor power spectrum results in

$$\Delta_t^2(k) = \left.\frac{2H^2}{\pi^2 M_{\rm pl}^2}\right|_{k=aH}. \tag{1.63}$$

As before the scale dependence is captured via *the tensor spectral index* that is defined as

$$n_t \equiv \frac{d\ln \Delta_t^2(k)}{d\ln k}, \quad \Delta_t^2(k) = A_t(k_*)\left(\frac{k}{k_*}\right)^{n_t}, \tag{1.64}$$

and may be written in terms of the slow roll parameters as

$$n_t = -2\epsilon_H. \tag{1.65}$$

Therefore, the tensor tilt is a direct measure of ϵ_H. Observational constraints on the amplitude of tensor perturbations are usually expressed in terms of *the tensor-to-scalar ratio*

$$r \equiv \frac{A_t}{A_s}, \tag{1.66}$$

which via the slow-roll parameter is written as $r = 16\epsilon_H$. It in turn provides the consistency relation for single field inflation models $r = -8n_t$. Its violation would be a signal of physics beyond the standard single-field approach. Currently n_t is constrained to be slightly red tilted and $r < 0.056$ at 95% confidence level by Planck 2018 results [53].

Therefore, inflation provides an irreducible SGWB. Observational constraints, however, lead to a very small amplitude of the GW power spectra. Denoting by $\Omega_{\rm GW}$ to be today's GW fractional energy density per logarithmic wave-number interval, its amplitude at CMB scales is of order at most $\Omega_{\rm GW} \sim 10^{-15}$. So small values are potentially detectable only for the next-to-next-generation of space-based observatories, for instance Big Bang Observatory (BBO) [112] or Deci-hertz Interferometer Gravitational wave Observatory (DECIGO) [113], as well as large surveys of stars such as Gaia [114, 115] and the upgrade THEIA (Telescope for Habitable Exoplanets and Interstellar/Intergalactic Astronomy)[116], see Figure 1.2. That is why there is a broad interest in alternative or complementary scenarios that could produce the stochastic GWs background at different levels, that are more likely to be detected during the next two decades.

One possibility to significantly enhance GW production within the inflationary framework, is the presence of a non-zero source term. In the early universe there are several possible sources for Π_{ij}^{TT}, coming from

- gauge fields,
- scalar field gradients,
- bulk fluid motion,
- gradients of second order scalar perturbations,

as well as other possibilities not listed here.

Another option is to break the space-time symmetries during inflation, the so-called space-reparametrization. In this case the graviton can acquire a mass which leads to the enhancement of tensor spectra at small scales, implying a blue tensor tilt. In addition to that, the brief but strong violation

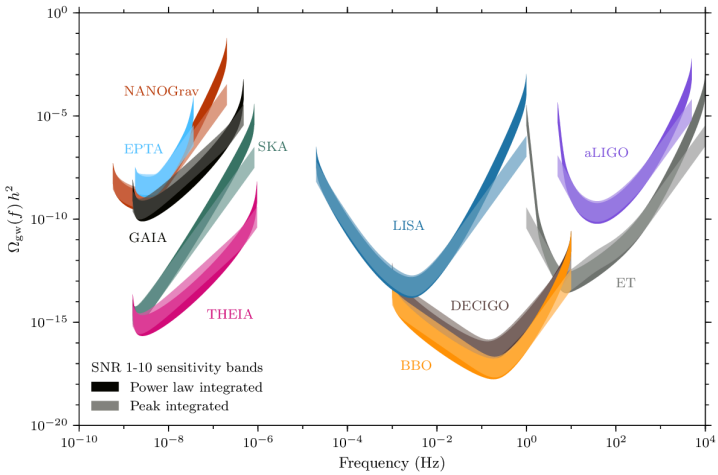

Figure 1.2: The sensitivity curves for different gravitational wave detectors, taken from [117].

of the slow-roll conditions may lead to a bump in the power spectra of scalar fluctuations, which imprints on $\Omega_{\rm GW}$. If the bump is big enough (at least 10^7 larger than its CMB value), this can also lead to the formation of primordial black holes. Besides inflation, the SGWB may be generated during (p)reheating. The non-perturbative particle production together with the non-linear-dynamics produce the GW background, which is unlike the one coming from inflation and has a peaked power-spectrum at very high-frequencies $f \sim 10^{10}$Hz [118]. Another possible cosmological origin for the SGWB may be cosmic strings, first order phase transitions and pre Big Bang models. From the astrophysical side, the SGWB may be generated for instance by binary black holes, binary neutron stars, other binary star systems, pulsars, magnetars and supernovae. For comprehensive reviews on cosmological backgrounds of gravitational waves and discussions of possible astrophysical sources see Ref. [119, 120] and references therein.

Now, the question arises: how to distinguish the cosmological origin of GWs from the astrophysical one? There are several "smoking guns" for the cosmological origin of SGWB, such as a non-Gaussian signal (the signal from astrophysical origin is Gaussian), chirality, anisotropy (intrinsic or induced) and a rich profile of GW power spectrum.

In Chapter 3 we will discuss the theoretical limitations on the chiral gravitational wave production sourced by spectator non-Abelian gauge fields during inflation, that can significantly enhance the tensor-to scalar ratio r while keeping the scalar spectral index n_s within the observational

bounds.

1.2.5 Upcoming experiments

One of the main goals in observational cosmology nowadays is to detect the primordial tensor fluctuations. Possible direction is polarization measurement of CMB. At the level of a few micro Kelvin the CMB is linearly polarized due to Thomson scattering of photons off free electrons just before decoupling. It was first observed by the Degree Angular Scale Interferometer (DASI) in 2002 [121] and was confirmed by many other experiments. The main idea of upcoming experiments is that scalar perturbations can only create polarization patterns of a particular type, parallel or perpendicular to the wave vector $\vec{k}$, that are called E-modes. If, in addition to that, a gravitational wave background is present, it would create an extra stretching of spacetime, which induces a polarization pattern that is rotated by a 45-degree angle and is called the B-mode polarization. Such polarization pattern cannot be produced by scalar fluctuations and hence, provides a unique signature of primordial gravitational waves. In addition to that, in some models with parity breaking, like Gauge-flation and Chromo-Natural inflation, gauge field tensor modes experience a transient growth in one of their polarizations, hence leading to production of chiral GWs. They could be potentially distinguishable from the standard vacuum fluctuations in future experiments, like CMB Stage-4 [122] and LiteBIRD [123], which aim to probe the tensor sector to values $r \simeq 0.001$.

Furthermore, CMB spectral distortions experiments like PIXIE, SuperPIXIE, Voyage 2050, 10×Voyage 2050 (see [124] for a recent review and references therein) aim to probe 10 e-folds of inflation further, that are not visible for CMB anisotropy measurements. Spectral distortions of the CMB spectrum occur because of dissipation of density perturbations through photon diffusion in the early universe, which is also called Silk damping. Such measurements will provide a unique test for departures from scale-invariance that, depending on the outcome, would support or disfavour a simple single-field inflationary scenario.

1.2.6 Open problems

Inflation nowadays is the leading framework for the early universe cosmology, that solves the horizon and flatness problems, and can produce density fluctuations that match the latest observational constraints. However, there are still some theoretical challenges that we outline below.

Since there is no UV complete theory of the early universe yet, inflation is an effective description that is valid until some cut-off scale $\Lambda < M_{\rm pl}$. Then the question should be asked: can the physics above this cut-off affect the low-energy dynamics during inflation? It turns out that corrections may affect the flatness of the potential. In particular, important corrections are of the form [125, 126] $\sum_n c_n V(\phi)\frac{\phi^{2n}}{\Lambda^{2n}}$, where c_n are dimensionless Wilson coefficients of order one. The major effect from these corrections is coming from the dimension-six operator $\Delta V = c_1 V(\phi)\frac{\phi^2}{\Lambda^2}$. When the inflaton value is smaller than the cut-off scale $\phi \ll \Lambda$, the correction is small $\Delta V \ll V$, however the second slow-roll parameter $\eta_V \ll 1$ gets significantly altered by this correction

$$\Delta\eta_V = \frac{M_{\rm pl}^2}{V}(\Delta V)'' \approx 2c_1\left(\frac{M_{\rm pl}}{\Lambda}\right)^2 > 1, \tag{1.67}$$

for $c_1 \sim 1$ and $\Lambda \lesssim M_{\rm pl}$. This issue is called *the eta problem*, that is present in most slow-roll models of inflation. One possible resolution is the presence of a shift symmetry for the inflaton field $\phi \to \phi + c$, which is the case in natural inflation [127].

The second problem is the problem of *initial conditions* for inflation, since it requires some fine-tuning of initial values for selected dynamics, see Ref. [128]. It includes *the overshoot problem*, meaning that for big initial velocities of the inflaton field, the flat region of the potential where inflation should happen may be overshot. It typically happens in small-field inflationary models, where field excursions $\Delta\phi$ are small in comparison to $M_{\rm pl}$. There the Hubble friction is not strong enough to decelerate the inflaton field. This is not the case for large-field models, where the Hubble friction is strong and leads to inflationary attractor solutions.

In addition to that, it was shown that inflation is past-geodesically incomplete [129–131], therefore some other physics is required to describe the past boundary of the inflating region of space-time, that is also called the singularity problem. This is resolved in alternatives to cosmological inflation, the so-called Bouncing cosmologies. In such models the universe never reaches a singularity, but instead undergoes a phase of contraction, that is followed by a bounce and a further expansion, that may repeat several times, see [132] for a review. Bouncing cosmologies have other problems, which, however, we will not pursue here.

Coming back to the inflationary framework and summing up its open problems, the legitimate questions arise: what happened before inflation has started or did inflation start at the top of the potential or somewhere

else? This questions are challenging and we hope that they will be answered in the forthcoming theoretical explorations.

1.3 Reheating

After the universe expanded at least e^{55} times, inflation has to end. Because of the enormous exponential expansion, the temperature of the universe also dropped considerably. However, in order for BBN to happen and meet the observable abundances of light elements, the universe has to be in a radiation-dominated state. This is the first and foremost motivation to assume, that between inflation and BBN, there was one more transition period that is called *reheating*. Below we outline the physics of this era, based mainly on Refs. [118, 133–136].

1.3.1 Reheating vs preheating

The necessity of the reheating mechanism was already clear after the first appearance of Guth's theory of inflation [27], which however lacked a "graceful exit", since collision of bubble walls does not lead to a thermal, homogeneous and isotropic universe. This was naturally resolved in the new inflation scenario proposed by Linde [28], where the reheating process was happening via the background oscillations of the inflaton field near the minimum of its potential. Historically, it was first described in 1982 *perturbatively* in works by Dolgov & Linde [137] and Abbott, Fahri & Wise [138] for the new inflation scenario. Soon after that new works devoted to reheating for various inflationary scenarios [139–142] started to appear.

The evolution of the inflaton field during the period of oscillations after inflation, see Figure 1.3, was described through the phenomenological equation

$$\ddot{\phi} + 3H(t)\dot{\phi} + \Gamma_{\rm tot}\,\dot{\phi} + V_\phi = 0, \tag{1.68}$$

where $\Gamma_{\rm tot}$ is the total decay width of the inflaton to daughter fields, which is calculated via quantum field theory (QFT) methods. The solution for $\phi(t)$ approaches the oscillatory regime and may be parametrised by

$$\phi(t) = \Phi(t)\sin\left(f(t)\,t\right), \tag{1.69}$$

where $\Phi(t)$ is the decreasing amplitude and $f(t)$ is the frequency of oscillations. The amplitude decays because of particle production as well as expansion of space. It may be written in the form

$$\Phi(t) = \Phi_0 e^{-\frac{1}{2}\Gamma_{\rm tot}t} e^{-\frac{1}{2}\int 3H\,dt}, \tag{1.70}$$

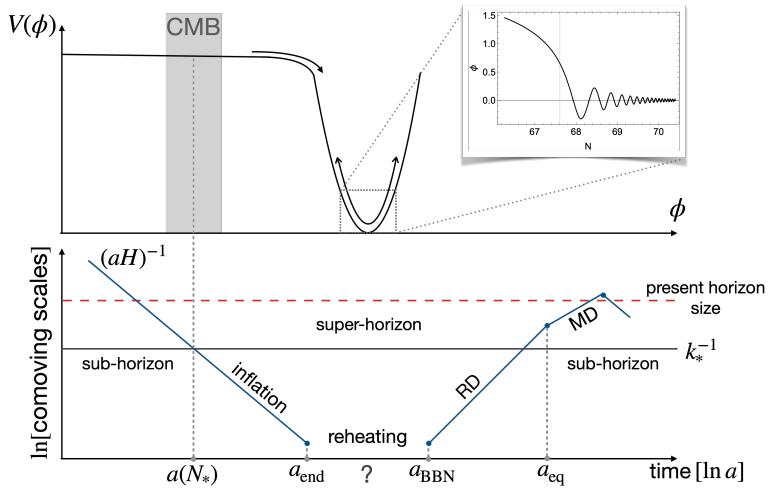

Figure 1.3: *Top panel:* The illustration of the inflation and reheating eras, as well as oscillations of the inflaton field ϕ around the minima of its potential $V(\phi)$, depending on the number of e-folds N from the start of inflation. The grey grid line in the $\phi - N$ inset corresponds to the moment of the end of inflation. The shaded grey region illustrates the perturbations during inflation that are visible in the CMB.
Bottom panel: Evolution of the Hubble radius $(aH)^{-1}$ (solid blue curve) and a representative fluctuation with comoving wave number k_* (solid grey line) in time. The red dashed line represents the present horizon size. RD and MD stand for the radiation dominated and matter dominated eras respectively. The scale factor $a(N_*)$ corresponds to the scale factor evaluated at the moment of horizon crossing of the representative mode, which happened at N_* e-folds starting from the beginning of inflation. Knowledge of N_* is crucial for the accurate determination of the CMB predictions, as will be discussed in detail in Section 1.3.4.1. Scale factors $a_{\rm end}, a_{\rm BBN}, a_{\rm eq}$ correspond to the moment of the end of inflation, start of the BBN and to the moment of matter and radiation equality respectively. The question mark symbolizes the unknown expansion history of the universe during the reheating era.

the precise values of which depend on the shape of the inflationary potential around its minimum. For instance, for a quadratic potential $V = \frac{1}{2}m^2\phi^2$ the oscillation amplitude equals $\Phi(t) \sim a^{-3/2}(t)\exp(-\Gamma_{\rm tot}t/2)$ and the frequency coincides with the inflaton mass $f(t) = m$.

In general, the equation of state of the reheating era highly depends on the shape of the potential near its origin. For polynomial behaviour $V \propto |\phi|^{2n}$, where n is not necessarily an integer number, however with the restriction $n > 1/2$ to ensure a non-singular first derivative at the minimum, the equation of state is given by [143]

$$\langle w \rangle \approx \frac{n-1}{n+1}. \tag{1.71}$$

This leads to a matter-dominated reheating era with $w = 0$ for quadratic potentials $n = 1$ and radiation-domination $w = 1/3$ for $n = 2$. The requirement $n > 1/2$ always leads to $w > -1/3$, which means that oscillations around minima of potential in any case lead to a decelerating stage of expansion. As we will see in Section 1.3.4.1, knowledge of the equation of state for the reheating era is crucial in order to provide accurate predictions for CMB observables.

However, such description appears to be incomplete. First of all, the perturbative description fails for large coupling constants which may easily emerge in the very early universe due to high energy scales. Secondly, in such description particle production becomes efficient when $H \lesssim \Gamma_{\rm tot}$, which is typically achieved only in a couple of e-folds after the end of inflation and may lead to a prolonged reheating era, that could change inflationary predictions and also affect BBN. The last and, perhaps, the most important reason is that it does not take into account the collective effects of the Bose condensate. Since the inflaton field at the end of inflation is a coherent wave, a condensate with a large occupation number of inflaton quanta that oscillate with the same phase around the minimum of its potential, the particle production should be described as a collective process. Due to large occupation numbers, the condensate itself may be treated as a classical field, however this is not the case for the decay products where a quantum description is required. Bose condensation effects may lead to exponential increase in particle production, that is impossible to capture via the perturbative analysis. This was realised by Traschen and Brandenberger in [144] and developed further in works by Dolgov & Kirilova, Shtanov and Kofman et al in [133, 145–149]. In these works it was proposed that reheating can proceed through *non-perturbative* processes, i.e. via parametric or tachyonic resonances. In the aforementioned and subsequent investigations, including lattice simulations [150], it turned out that in many inflationary models the first stages of reheating were dominated by the parametric resonance, hence in order to distinguish this stage from the slow perturbative description it was named *preheating*. Despite of this, the perturbative treatment is still used in the final stages of the reheating era, to complete the transfer of energy after the shut down of a resonance.

To better understand the essence of preheating, let us consider the static universe approximation, i.e. $H(t) = 0$. Without specifying the interaction term for now, let χ be the daughter scalar field that is produced via inflaton oscillations. As discussed above, χ should be treated as a quantum field and considered as a fluctuation to the classical oscillating inflaton background.

In the Heisenberg representation it is written as

$$\hat{\chi}(t,\mathbf{x}) = \frac{1}{(2\pi)^3}\int d^3k \left(\hat{a}_k\chi_k(t)e^{-i\mathbf{kx}} + \hat{a}_k^\dagger\chi_k^* e^{i\mathbf{kx}}\right). \tag{1.72}$$

Fluctuations start to evolve from their vacuum state, since inflation washed out all possible initial particle densities to negligible values. Then, the equation of motion for each mode k in the static universe approximation may be written in the form

$$\ddot{\chi}_k + \omega^2(k,t)\chi_k = 0, \tag{1.73}$$

which describes an oscillator with a time-dependent and periodic frequency. In particular, for the trilinear model where the interaction between the inflaton field ϕ and the daughter scalar field χ is given by $V_{\phi,\chi} = m^2\phi^2/2 + m_\chi^2\chi^2/2 + \sigma\phi\chi^2$, the frequency is equal to $\omega^2(k,t) = k^2 + m_\chi^2 + 2\sigma\phi(t)$, with m_χ being the mass of χ. The equation (1.73) for a periodic $\omega(k,t)$ is known as *Hill's equation*, which, according to the Floquet theorem [151], admits the general solution

$$\chi_k(t) = e^{\mu_k t}\mathcal{P}_{k+}(t) + e^{-\mu_k t}\mathcal{P}_{k-}(t). \tag{1.74}$$

Here $\mathcal{P}_{k\pm}(t) = \mathcal{P}_{k\pm}(t+T)$ are periodic with period T. The quantity μ_k is called *the Floquet exponent*. If the real part of the Floquet exponent is non-zero, the mode function χ_k experiences an exponential growth and parametric resonance happens. In addition to that, if $\omega(k,t)$ is a harmonic function, Hill's equation may be reduced to *the Mathieu equation*

$$\chi_k'' + (A_k - 2q\cos 2z)\chi_k = 0, \tag{1.75}$$

where the prime derivative corresponds to "a new time coordinate z". For instance, in the trilinear model $A_k = 4(k^2 + m_\chi^2)/m^2$, $q = 4\sigma\Phi(t)/m^2$, $z = mt/2$. Then the number density of created particles will be given by

$$n_k \sim |\chi_k|^2 = e^{2\mu_k z}. \tag{1.76}$$

The stability and instability regions of the Mathieu equation are very well known [152], which allows us to determine regions in parameter space where modes experience the exponential amplification that leads to the bursts in particle production, see Figure 1.4.

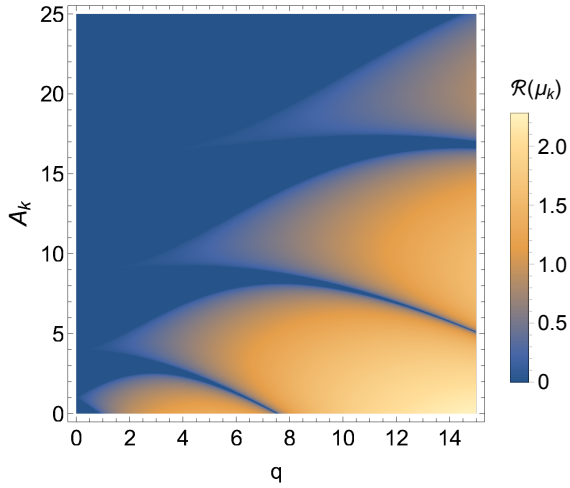

Figure 1.4: Instability chart of the Mathieu equation. Here A_k is the constant offset and q is the amplitude of oscillations in the Mathieu equation (1.75). Regions in blue correspond to the stability bands, while yellow correspond to the instability bands with values of the Floquet exponent $\mathcal{R}(\mu_k) > 0$ shown at the bar legend on the right.

1.3.2 Narrow and broad resonance

It is well known [152] that the Mathieu equation (1.75) has two different regimes of the parametric resonance: narrow and broad resonances. As could be guessed from its name, *a narrow* resonance occurs only in some narrow bands $A_k \simeq l^2$, with $l = 1, 2, \ldots$, for small oscillation amplitudes, meaning for $|q| \ll 1$ (for $A_k > 0$), see Figure 1.4. Hence, only a very narrow range of modes with corresponding wave-numbers Δk get exponentially excited, while modes with the remaining wave numbers stay in the vacuum state and can be produced through perturbative decays. Such resonance eventually stops because of two reasons. The first reason is the decay of the oscillation amplitude $\Phi(t)$ that in turn determines the behaviour of the parameter q and the Floguet exponent μ_k. According to (1.70), $\Phi(t)$ decays because of both perturbative decay as well as the expansion of space. Hence, the narrow parametric resonance will stop when the perturbative decay becomes efficient. The second reason is that the physical momenta redshift as $k_{\rm phys} = k/a$, hence initially resonant bands Δk will very quickly redshift away and the narrow resonance will eventually finish.

A broad resonance happens when the amplitude of oscillations is large. This corresponds to the regime $|q| \gtrsim 1$. In this case a broad, continuous range of modes with wave numbers k get excited and thus the broad reso-

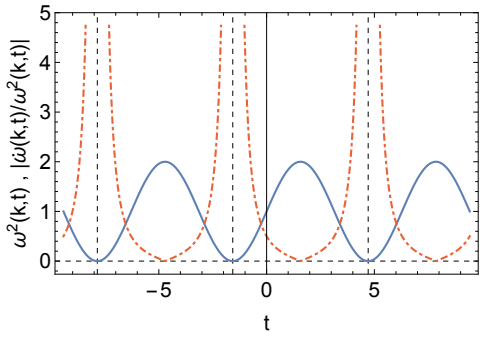

Figure 1.5: Illustration of the violation of the adiabaticity condition. The blue solid curve shows the frequency $\omega^2(k,t)$, while the red dot-dashed line illustrates the violation of the adiabaticity condition (1.77) at points with $\omega^2(k,t)=0$.

nance is much more efficient than the narrow one. The particle production happens in bursts, at the points of maximum acceleration of the inflaton field when *the adiabaticity condition* is *violated*, i.e. when

$$\left|\frac{\dot{\omega}(k,t)}{\omega^2(k,t)}\right| \gg 1. \tag{1.77}$$

The adiabaticity condition violation (1.77) holds when the interaction term inside $\omega^2(k,t)$ vanishes, which happens twice per period, making the particle production rate to be comparable to the inflaton period of oscillations T, see Figure 1.5. Let us note that for the narrow resonance the adiabaticity condition is satisfied all the time, because the oscillation amplitude is small and hence the oscillation frequency is approximately constant $\omega^2(k,t)\approx k^2=\text{const}$ and particle production happens continuously.

It turns out that physics of the broad parametric resonance reduces to the partial waves scattering off successive inverted parabolic potentials. To understand better why this is the case, let us write down solutions to the (1.73) when the adiabaticity condition is satisfied, i.e. in *the Wentzel–Kramers–Brillouin (WKB) approximation*

$$\chi_k(t)=\frac{\alpha_k(t)}{\sqrt{2\omega(k,t)}}e^{-i\int\omega(k,t)dt}+\frac{\beta_k(t)}{\sqrt{2\omega(k,t)}}e^{i\int\omega(k,t)dt}, \tag{1.78}$$

where $\alpha_k(0)=1$, $\beta_k(0)=0$ are the Bogolyubov coefficients. The occupation numbers are then expressed as

$$n_k(t)=|\beta_k(t)|^2. \tag{1.79}$$

Let us define the points t_j where the frequency $\omega^2(k,t)$ has a minimum and the adiabaticity condition is violated. We may expand the frequency of oscillations around t_j as

$$\omega^2(k,t) = \omega^2(k,t_j) + \omega^{2''}(k,t_j)(t-t_j)^2 + \cdots , \tag{1.80}$$

with $\omega^{2''}(k,t_j) = \left.\frac{d\,\omega^2(k,t)}{dt}\right|_{t=t_j}$. In terms of new variables that are defined as

$$\tilde{\eta} \equiv \left(2\omega^{2''}(k,t_j)\right)^{1/4}(t-t_j), \quad \tilde{\kappa}^2 \equiv \frac{\omega^2(k,t_j)}{\sqrt{2\omega^{2''}(k,t_j)}}, \tag{1.81}$$

the evolution equation for the mode functions (1.73) may be rewritten in the form

$$\frac{d^2\chi_k}{d\tilde{\eta}^2} + \left(\tilde{\kappa}^2 + \frac{\tilde{\eta}^2}{4}\right)\chi_k = 0. \tag{1.82}$$

This is the Schrödinger equation for a wave function scattering in an inverted parabolic potential with solutions being the parabolic cylinder functions $W(\tilde{\kappa}^2, \pm\tilde{\eta})$. Hence, indeed, the broad resonance problem is replaced by the partial waves scattering on inverted parabolic potentials.

Before t_j the WKB approximation is valid, hence the solution for mode functions is given by (1.78) with the Bogolyubov coefficients α_k^j, β_k^j. After the scattering at t_j has already happened, the wave $\chi_k(t)$ again takes the form of (1.78) but now with $\alpha_k^{j+1}, \beta_k^{j+1}$. The relation between ingoing and outgoing waves may be found via the relation for the Bogolyubov coefficients, that are expressed through the reflection R_k and transmission D_k coefficients as

$$\begin{pmatrix} \alpha_k^{j+1} e^{-i\theta_k^j} \\ \beta_k^{j+1} e^{+i\theta_k^j} \end{pmatrix} = \begin{pmatrix} \frac{1}{D_k} & \frac{R_k^*}{D_k^*} \\ \frac{R_k}{D_k} & \frac{1}{D_k^*} \end{pmatrix} \begin{pmatrix} \alpha_k^j e^{-i\theta_k^j} \\ \beta_k^j e^{+i\theta_k^j} \end{pmatrix}, \tag{1.83}$$

where $\theta_k^j = \int_0^{t_j} \omega(k,t)dt$ is the accumulated phase until the jth scattering. To satisfy the properties of the Bogolyubov coefficients, the reflection and transmission coefficients satisfy the usual relation $|R_k|^2 + |D_k|^2 = 1$. Assuming the daughter field χ_k was in the vacuum state at the beginning, its occupation numbers after $(j+1)$ scatterings may be written as

$$n_k^{j+1} = \left|\frac{R_k^j}{D_k^j}\right|(n_k^j+1)\left|\frac{1}{D_k^j}\right|^2 n_k^j + 2\left|\frac{R_k^j}{D_k^j D_k^{j*}}\right|\sqrt{n_k^j(n_k^j+1)}\cos(\theta_k^j + \Delta\theta_k^j), \tag{1.84}$$

with $\Delta\theta_k^j = \arg(R_k^j \alpha_k^j \beta_k^{j*})$.

Let us briefly describe the properties of the result (1.84). As was already mentioned before, the occupation numbers grow as a step-like function of time, staying constant between successive scatterings, because there the oscillation amplitude is approximately constant. In addition to that, such behaviour of occupation numbers cannot be captured perturbatively, since (1.84) depends on the coupling as $\sim e^{-1/g}$, and hence becomes non-analytical at $g = 0$, with g being some coupling constant. For $n_k^j \gg 1$ the occupation number of created particles grows exponentially because of the effects of the Bose-Einstein statistics. In that case from (1.84) we find $n_k^{j+1} = e^{2\mu_k^j} n_k^j$ and the Floquet exponent μ_k^j may be expressed as

$$\mu_k^j = \ln \left| \frac{1 + |R_k^j| e^{i(\theta_k^j + \Delta\theta_k^j)}}{\sqrt{1 - |R_k^j|^2}} \right|. \tag{1.85}$$

Because of the presence of the accumulated phase $\theta_k^j + \Delta\theta_k^j$, the incoming and outgoing waves may add up constructively or destructively. This leads to a particular *band structure* in Floquet charts.

The analysis above was performed in the static universe approximation. In most cases the expansion of the universe may be taken into account by changing the variables to $X_k(t) = f[a(t)]\chi_k(t)$, where $f[a(t)]$ is a function of the scale factor $a(t)$, which leads to the equation of motion for the mode functions of the form

$$\ddot{X}_k + \left[\omega^2(k,t) + \Delta\right] X_k = 0, \tag{1.86}$$

where the dot derivative is taken with respect to cosmic time t. Here Δ depends on the scale factor $a(t)$ and may be interpreted as an additional phase. In some cases this phase that is coming from the expansion of the universe may exactly compensate the phase acquired in a scattering, leading to the destructive interference and decrease in the number of particles in that mode. This leads to the stochastic evolution of the particle number and is known as *stochastic preheating*. The general condition for significant particle production is the requirement that the growth rate of fluctuations is much larger than the rate of expansion, that is written as

$$\frac{|\mathrm{Re}(\mu_k)|}{H} \gg 1. \tag{1.87}$$

1.3.3 Multi-field preheating

In this section we will discuss the physics of preheating in multi-field models with non-trivial field-space manifolds. Similarly to the single-field case presented above, the primary question for investigation is the evolution of fluctuations. For multiple field case such formalism was developed and applied in [34, 35, 37, 136, 153].

1.3.3.1 Perturbations and mass scales

To start with, the perturbations $\delta\phi^I(x^\mu)$ to the background field trajectories $\varphi^I(t)$ may be written in the form of the gauge-invariant Mukhanov-Sasaki variable $Q^I \equiv \delta\phi^I + \frac{\dot\phi^I}{H}\psi$ that satisfies the equation of motion (1.55) with the mass-squared matrix $\mathcal{M}^I_{\ J}$ defined in (1.56), as was discussed in Section 1.2.4.3. The next step is the quantisation procedure and analysis of resulting perturbations, which is rather cumbersome even for the two field case. Below we will outline this procedure and focus on the case involving two scalar fields that converge to the single-field attractor along geodesic, which is the main topic of the Part II of the thesis.

To perform the quantisation, it is convenient to introduce another set of variables $Q^I(x^\mu) \to X^I(x^\mu)/a(t)$ and change cosmic time to conformal time $d\tau = dt/a(t)$. Next we need to quantize the fields X^I. In the two-field case, let us define the fields as ϕ and χ, hence the corresponding operators $\hat X^\phi$ and $\hat X^\chi$ for the general case of the field-space metric may be written as [136]

$$\hat X^\phi(x^\mu) = \int \frac{d^3k}{(2\pi)^{3/2}} \left[\left(v_k e_1^{\ \phi} \hat a_k + c_k e_2^{\ \phi} \hat b_k \right) e^{i\mathbf{kx}} + \left(v_k^* e_1^{\ \phi} \hat a_k^\dagger + c_k^* e_2^{\ \phi} \hat b_k^\dagger \right) e^{-i\mathbf{kx}} \right], \tag{1.88}$$

$$\hat X^\chi(x^\mu) = \int \frac{d^3k}{(2\pi)^{3/2}} \left[\left(y_k e_1^{\ \chi} \hat a_k + z_k e_2^{\ \chi} \hat b_k \right) e^{i\mathbf{kx}} + \left(y_k^* e_1^{\ \chi} \hat a_k^\dagger + z_k^* e_2^{\ \chi} \hat b_k^\dagger \right) e^{-i\mathbf{kx}} \right], \tag{1.89}$$

where $\hat a, \hat b_k, \hat a_k^\dagger, \hat b_k^\dagger$ are creation and annihilation operators, v_k, c_k, y_k, z_k are associated mode functions, and e_a^I with $I = \phi, \chi$, $a = 1, 2$ are components of the vielbein in the field space, defined as

$$\delta^{bc} e_b^I(\tau) e_c^{\ J}(\tau) = \mathcal{G}^{IJ}(\tau). \tag{1.90}$$

For such general case of the field-space metric, the resulting equations for the mode functions appear to be in the form of two systems of two coupled

equations where v_k couples with y_k, and c_k with z_k:

$$\begin{aligned}
&\left(v_k'' + \omega_\phi^2(k,\tau)v_k\right) e_1^{\ \phi} = -a^2 \mathcal{M}^\phi_{\ \chi} y_k e_1^{\ \chi}, \quad \left(c_k'' + \omega_\phi^2(k,\tau)c_k\right) e_2^{\ \phi} = -a^2 \mathcal{M}^\phi_{\ \chi} z_k e_2^{\ \chi}, \\
&\left(y_k'' + \omega_\chi^2(k,\tau)y_k\right) e_1^{\ \chi} = -a^2 \mathcal{M}^\chi_{\ \phi} v_k e_1^{\ \phi}, \quad \left(z_k'' + \omega_\chi^2(k,\tau)z_k\right) e_2^{\ \chi} = -a^2 \mathcal{M}^\chi_{\ \phi} c_k e_2^{\ \phi}.
\end{aligned} \tag{1.91}$$

Here $\mathcal{M}^I_{\ J}$ defined in (1.56) and

$$\begin{aligned}
\omega_\phi^2(k,\tau) &\equiv k^2 + a^2(\mathcal{M}^\phi_{\ \phi} - \frac{1}{6}R), \\
\omega_\chi^2(k,\tau) &\equiv k^2 + a^2(\mathcal{M}^\chi_{\ \chi} - \frac{1}{6}R).
\end{aligned} \tag{1.92}$$

We will focus our attention on the case where at the beginning of reheating the background motion is geodesic. Without loss of generality this assumes the attractor solution along $\chi = 0$, which may be always achieved upon rotation $\phi^I \to \phi^{I'}$, see [136] for the detailed discussion. This behaviour is common in models of inflation with non-minimal coupling to gravity that are called ξ-attractors [154, 155] and include Higgs inflation [156, 157], and models with hyperbolic field-space geometry, like α-attractors [50–52, 61]. With such a choice the cross-terms in $\mathcal{G}_{IJ}$ and $\mathcal{M}^I_{\ J}$ vanish and the field space vielbein becomes diagonal

$$e_a^{\ I} \to \begin{pmatrix} e_1^{\ \phi} & 0 \\ 0 & e_2^{\ \chi} \end{pmatrix}, \tag{1.93}$$

with $e_2^{\ \phi} \sim e_1^{\ \chi} \sim 0$, $e_1^{\ \phi} e_1^{\ \phi} \simeq \mathcal{G}^{\phi\phi}$, $e_2^{\ \chi} e_2^{\ \chi} \simeq \mathcal{G}^{\chi\chi}$ and $\mathcal{G}_{\phi\phi}\mathcal{G}^{\phi\phi} = \mathcal{G}_{\chi\chi}\mathcal{G}^{\chi\chi} = 1 + \mathcal{O}(\chi^2)$. Because $\mathcal{M}^\phi_{\ \chi} \sim \mathcal{M}^\chi_{\ \phi} \sim 0$ the source term in (1.91) is zero, that decouples mode functions v_k and z_k, while setting the remaining two to zero $c_k \sim y_k \sim 0$. Therefore, the equations for scalar mode functions reduce to the familiar case of two independent harmonic oscillator equations with time-dependent frequency

$$\begin{aligned}
&\partial_\tau^2 \phi_k + \omega_\phi^2(k,\tau)\phi_k \simeq 0, \quad \omega_\phi^2(k,\tau) \equiv k^2 + a^2 m^2_{\text{eff},\phi}(\tau), \\
&\partial_\tau^2 \chi_k + \omega_\chi^2(k,\tau)\chi_k \simeq 0, \quad \omega_\chi^2(k,\tau) \equiv k^2 + a^2 m^2_{\text{eff},\chi}(\tau).
\end{aligned} \tag{1.94}$$

Here, we have denoted mode functions as $v_k \equiv \phi_k$ and $z_k \equiv \chi_k$ to indicate the clear relation with each field perturbation. The effective masses for each fluctuation have four different contributions:

$$m^2_{\text{eff},I} = m^2_{1,I} + m^2_{2,I} + m^2_{3,I} + m^2_{4,I}, \tag{1.95}$$

with $I = \phi, \chi$. Different terms are defined as

$$\begin{aligned} m^2_{1,\phi} &\equiv \mathcal{G}^{\phi K}\left(\mathcal{D}_\phi \mathcal{D}_K V\right), \\ m^2_{2,\phi} &\equiv -\mathcal{R}^{\phi}_{\ LM\phi}\dot{\varphi}^L\dot{\varphi}^M, \\ m^2_{3,\phi} &\equiv -\frac{1}{M^2_{\rm pl}a^3}\delta^{\phi}_{\ K}\delta^{J}_{\ \phi}\,\mathcal{D}_t\left(\frac{a^3}{H}\dot{\varphi}^K\dot{\varphi}_J\right), \\ m^2_{4,\phi} &\equiv -\frac{1}{6}R = (\epsilon - 2)H^2\,, \end{aligned} \tag{1.96}$$

with identical contributions to $m^2_{{\rm eff},\chi}$ but with $\phi \leftrightarrow \chi$. Here $m^2_{1,I}$ is the Hessian of the potential in a curved field space defined by the field metric $\mathcal{G}^{IJ}$. The second term $m^2_{2,I}$ demonstrates the geodesic deviation of the two trajectories caused by the non-trivial field-space geometry. The third term $m^2_{3,I}$ encodes turning of the trajectory and the last contribution $m^2_{4,I}$ shows the changes in the background space-time via the presence of the space-time curvature R.

For the particular choice of the two-field α-attractor model [158, 159], with the attractor solution along $\chi = 0$, effective masses simplify to

$$m^2_{{\rm eff},\phi} \simeq V_{\phi\phi}(\chi = 0) \tag{1.97}$$

$$m^2_{{\rm eff},\chi} \simeq V_{\chi\chi}(\chi = 0) + \frac{1}{2}\mathcal{R}\dot{\phi}^2, \tag{1.98}$$

where the field space Ricci curvature scalar $\mathcal{R}$ is parametrised by the dimensionless parameter α as $\mathcal{R} = -4/3\alpha$. From here one can see that $m^2_{{\rm eff},\phi}$ is always positive, since it is determined by the Hessian of the potential near the minimum $V_{\phi\phi}(\chi = 0) > 0$. It means that the inflaton field ϕ in some regions of parameter space may preheat through the parametric resonance described in detail in Section 1.3.1. However, for χ perturbations and $m^2_{{\rm eff},\chi}$, the situation is different. In the case of α-attractors, the field space is a negatively curved manifold and hence the Ricci curvature scalar always takes negative values. It means that, depending on the interplay between the potential $V_{\chi\chi}$ and curvature $\frac{1}{2}\mathcal{R}\dot{\phi}^2$ terms, the effective mass $m^2_{{\rm eff},\chi}$ may take both positive and negative values. If $m^2_{{\rm eff},\chi}$ becomes negative, the perturbations of the χ field rapidly experience exponential amplification caused by the tachyonic resonance and the system quickly reaches the radiation-dominated equation of state $w \simeq 1/3$, as was shown in lattice simulations [160].

Remarkably, the instability bands are easily parametrised by the one parameter α that determines the value of the field space curvature, as well

as observational predictions such as the tensor-to-scalar ratio. In particular, the term $\frac{1}{2}\mathcal{R}\dot{\phi}^2 \propto -\frac{1}{\alpha}\left(\frac{\sqrt{\alpha}}{\mathcal{O}(1)}\right)^2 = -\mathcal{O}(1)$ stays almost the same and does not react to the changes in the field curvature from different values of α. However, this is not the case for the Hessian of the potential $V_{\chi\chi}$. First of all, the potential term does not scale so uniformly with α and, in addition to that, the cases with symmetric and asymmetric potentials appear to be very different. Here we refer to the symmetry/asymmetry of the potential near its minimum, that is relevant for classification of the reheating behaviour.

Let us start with describing the case with *symmetric* two-field α -attractor potential. For such a choice, for any value of $\alpha \lesssim 10^{-4}$ and the potential steepness n, the curvature term (1.98) always dominates over the Hessian of the potential. For any wave number that is smaller than a maximally amplified wave number $k_{\max}$, determined by $\omega_\chi^2(k_{\max}, \tau) = 0$, the effective frequency $\omega_\chi^2(k_{\max}, \tau)$ is negative, which leads to the tachyonic resonance.

Instead, the choice of *asymmetric* potentials distinguishes two distinct sub-cases. The first one corresponds to *massive fields*, meaning that around the global minimum at $\phi = \chi = 0$ the Hessian of the potential $V_{\chi\chi} > 0$, which happens for potentials with steepness $n = 1$. For higher potential steepness $n > 1$ the potential gradient $V_{\chi\chi} = 0$, and hence corresponds to the case with *massless fields*.

The massless field case leads to the dominance of the negative field space curvature contribution over the positive potential one in (1.98). This results in a negative effective mass square $m^2_{\text{eff},\chi} < 0$ and the outbreak of tachyonic resonance, starting at values $\alpha \approx 10^{-3}$.

By contrast, for massive fields the potential contribution always dominates over the field curvature term, making $m^2_{\text{eff},\chi} > 0$. Hence, in such case both perturbations of ϕ and χ fields may be amplified via parametric resonance, while more efficient tachyonic resonance does not happen. It turns out that for massive potentials and bigger values of α (or equivalently smaller field-space curvatures), the parametric resonance is stronger for $\delta\phi$ perturbations than for $\delta\chi$ in comparison to the case with symmetric potentials. This happens at values $\alpha \approx 10^{-3}$ where the same model with symmetric potential and any potential steepness does not reheat at all.

Therefore, the two-field α -attractor model with asymmetric potential reheats efficiently in a region of parameter space which is absolutely inefficient when the symmetric potential is chosen. This is the crucial finding, since, as will be discussed in Section 1.2.4, inefficient reheating may lead to a prolonged matter-dominated phase after inflation, change the time when

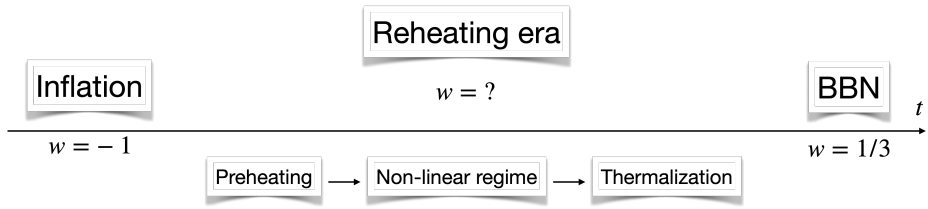

Figure 1.6: The illustration of stages of the reheating era.

CMB modes exit the horizon and thus shift CMB predictions. The complete analysis of scaling properties and their universality that determine the preheating efficiency is discussed in Chapter 4. It is followed by an extensive investigation of the symmetry properties for the two-field inflationary potentials and their implications for the duration of the reheating era, presented in Chapter 5 of the thesis.

1.3.4 Observational signatures from the reheating era

The preheating process, outlined above, does not describe the complete transition of the universe to the thermal state, as illustrated in Figure 1.6. Instead, it is followed by the non-linear regime, during which various non-trivial field configurations may be formed, such as oscillons, Q-balls, solitons and topological defects, like domain walls and metastable global cosmic strings. After the non-linear phase the turbulent scaling occurs, which is characterized by a slow transfer of energy to both ultraviolet and infrared modes, and completed by the process of thermalization, which brings all degrees of freedom into kinetic and chemical equilibrium and the spectrum to a thermal distribution.

There are several complications in extracting observational constraints for the reheating era. First of all, the details of dynamics on subhorizon scales is hidden by later, non-linear evolution of cosmic structure on short scales. Hence, it is not possible to extract the effect on the curvature perturbation from the CMB. Secondly, the thermalization process completely washes away the details of the earlier stages of the reheating era. Nevertheless, there are some very important observational implications of the reheating era, that we will outline below.

1.3.4.1 CMB predictions and reheating

The first indirect manifestation is related to the expansion history of the universe during the reheating era. As was discussed in Section 1.3.1 and, in particular, shown by the equation (1.71), there is a high uncertainty in the equation of state w during reheating. It is extremely important, since the expansion history highly influences the CMB predictions, as it changes the time of mapping of the inflationary perturbation modes from the horizon exit to its re-entry, see Figure 1.3. It was shown [161] that the number of e-folds N_* from the end of inflation to the pivot scale $k_* = a_* H_*$, where the modes cross the horizon, is related to the expansion history of the universe as follows

$$\frac{k_*}{a_0 H_0} = e^{-N_*} \frac{a_{\rm end}}{a_{\rm reh}} \frac{a_{\rm reh}}{a_{\rm eq}} \frac{H_*}{H_{\rm eq}} \frac{a_{\rm eq} H_{\rm eq}}{a_0 H_0}, \tag{1.99}$$

where the subscripts "$*, {\rm end}, {\rm reh}, {\rm eq}, 0$" denote that quantities are evaluated at the pivot scale, at the end of inflation, at the end of reheating, at the moment when radiation and matter densities are equal and at the present moment of time respectively. This relation may be further rewritten [162, 163] (see also Ref. [135] for more detailed discussion) as

$$N_* = 66.89 - \ln \frac{k_*}{a_0 H_0} + \frac{1}{4} \ln \frac{V_*^2}{M_{\rm pl}^4 \rho_{\rm end}} + \frac{1}{12} \ln \left[\frac{1}{g_{\rm th}} \left(\frac{\rho_{\rm th}}{\rho_{\rm end}} \right)^{\frac{1-3\bar{w}_{\rm int}}{1+\bar{w}_{\rm int}}} \right], \tag{1.100}$$

where $\rho_{\rm th}, g_{\rm th}$ are the energy density and the number of relativistic degrees of freedom respectively at thermalization and V_* is the inflationary potential at the pivot point, defined by $V_* = V_*(\{q_i\}, \phi_*)$ where $\{q_i\}$ are the parameters entering the inflaton potential $V = V(\{q_i\}, \phi)$. The mean equation of state $\bar{w}_{\rm int} > -1/3$ between the end of inflation and complete thermalization is defined as

$$\bar{w}_{\rm int} \equiv \int_{t_{\rm end}}^{t_{\rm th}} \frac{w(t) dt}{t_{\rm th} - t_{\rm end}}. \tag{1.101}$$

One of the parameters in the potential may be fixed from the measured amplitude of scalar perturbations A_s. Hence, from (1.100), it turns out that N_* may be parametrised by the following set of parameters

$$N_* = N_* \left(\{q_i - 1\}, A_s, \rho_{\rm th}^{\frac{1-3\bar{w}_{\rm int}}{1+\bar{w}_{\rm int}}} / g_{\rm th} \right). \tag{1.102}$$

In turn, the N_* parametrises the CMB observables as

$$n_s = n_s(N_*, \{q_i - 1\}), \quad r = r(N_*, \{q_i - 1\}). \tag{1.103}$$

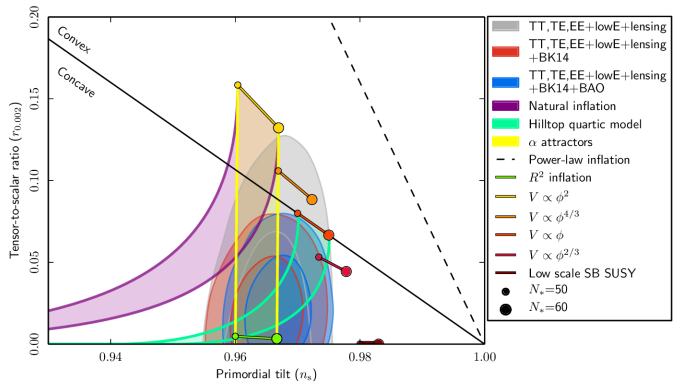

Figure 1.7: 68 % and 95 % confidence level regions for n_s and r from Planck, together with theoretical predictions of inflationary models [53].

Currently, every figure that confronts model-dependent inflationary predictions with Planck constraints for n_s and r, contains the theoretical uncertainty in N_*, since its precise value is not known and is typically set to 50 and 60 e-folds. This uncertainty is so big, that takes nearly one half of the 1σ contour in $n_s - r$ plane, see Figure 1.7. Therefore, knowledge of the equation of state $\bar{w}_{\rm int}$, as well as the energy scale $\rho_{\rm th}$ and the time of thermalization $a_{\rm th}$ which is specified by $g_{\rm th}$, are crucial for the accurate determination of N_* and correct comparison of inflationary predictions with the CMB observations.

The development of the Effective Field Theory of preheating would help to provide an easy determination of the reheating efficiency together with the number of e-folds N_*, leading to reducing the error bars in the $n_s - r$ plane. This would allow us to rule out many inflationary models that, because of huge uncertainties, still match the Planck constraints. In Chapter 4, 5 we identify the important mass scales that control the tachyonic growth of fluctuations and determine the resonance efficiency, taking a first step towards an Effective Field Theory description of preheating in hyperbolic manifolds.

1.3.4.2 Stochastic gravitational wave background from reheating

The idea that non-linear processes during the reheating era can generate a stochastic gravitational wave background was first studied in [164] and further developed in subsequent works [165–176]. The GW background coming from reheating is generated from the classical evolution of inhomogeneities

on sub-horizon scales, whereas the origin of the inflationary background is purely quantum, as was discussed in Section 1.2.4.4. That is why the power spectra from reheating appear to be peaked, unlike the almost scale-invariant tensor spectra from single field inflation. The peak frequency may be determined by the scale where the inflaton condensate is substantially fragmented (or destroyed). This happens when the back-reaction effects become important. The peak frequency f_0 of the gravitational energy density $\Omega_{\rm GW}$ per logarithmic frequency interval depends on the wave number and the Hubble scale as follows $f_0 \propto \frac{k}{\sqrt{M_{\rm pl}H}}$ [167, 177]. Typically $k \propto H$, hence the peak frequency is equal to [118, 135]

$$f_0 \sim \beta^{-1}\sqrt{\frac{H_{\rm br}}{M_{\rm pl}}} \times 4 \times 10^{10}{\rm Hz}, \quad \Omega_{\rm GW} \sim 10^{-6}\beta^2, \tag{1.104}$$

where $H_{\rm br}$ is the Hubble rate at back-reaction. The constant factor β is usually of the value $10^{-2} - 10^{-3}$ and is estimated from a linear analysis of the instabilities. This leads to typical frequencies $f_0 \sim 10^{10} - 10^{11}$Hz and amplitudes of the GW energy density $\Omega_{\rm GW} \sim 10^{-10} - 10^{-12}$, which is far from the observable ranges of contemporary GW detectors, that can measure frequencies at most $f_0 \sim 10^3 - 10^4$Hz, see Figure 1.2. For smaller values of $H_{\rm br}$, the peak frequency moves towards the observable range, however the smallness of the GW amplitude $\Omega_{\rm GW}$ leaves it currently inaccessible to direct detection.

1.3.4.3 Baryon asymmetry and relics

When the particle energies in the expanding universe become too small to create new pairs, almost all particles and antiparticles annihilate each other. However, a small amount of matter does not annihilate and leads to the remnant matter density that is observable today. This is the essence of *the baryon asymmetry problem*. Baryon asymmetry may be defined as the ratio between the difference of baryon n_B and antibaryon $n_{\bar{B}}$ number density to the photon number density n_γ

$$\tau \equiv \frac{n_b}{n_\gamma} \approx 6 \times 10^{-10}, \tag{1.105}$$

where $n_b = n_B - n_{\bar{B}}$ and $n_\gamma \sim n_B + n_{\bar{B}}$. This asymmetry has no explanation within the Standard Model (SM) and is one of the observational signatures of physics beyond it [178].

Hence, to explain the baryon asymmetry there should be new physics, that should meet Sakharov's conditions [179]: (i) non-conservation of the baryon number, (ii) violation of C and CP invariance; (iii) deviation from thermal equilibrium. Since during the reheating era particles are produced non-perturbatively and out of thermal equilibrium, with off-shell processes during the thermalisation stage, the reheating era is of a particular interest for a better understanding of the baryon asymmetry problem. In various studies [180–188] it was shown that indeed the non-linear dynamics during reheating can highly influence the generation of the baryon asymmetry.

In addition to that, the non-linear dynamics of reheating can lead to fragmentation of the inflaton condensate and to the formation of stable localized configurations. Some of these configurations, such as oscillons, can stay stable for millions of inflaton oscillations and as a result lead to a prolonged matter-dominated phase after inflation that may alter observational predictions and also delay BBN. In addition to that, oscillon formation may generate features in tensor power spectra at specific wavenumbers, as was discussed in [189]. Large inhomogeneities can also form primordial black holes, that would induce a matter-dominated expansion history during the reheating era. Moreover, self-interactions may lead to nongravitational dark matter structure growth resulting in compact halos, leading to several observational signatures [190]. Last but not least, the reheating era may play an important role in primordial magnetogenesis [191–194].

1.4 Work in this thesis

This thesis consists of two parts. Part I investigates inflation with multiple fields together with emerging observational consequences for scalar and tensor power spectra. Part II is focused on multi-field reheating, its efficiency and duration in curved field-space manifolds.

- **Part I. Multi-field inflation.**

  Chapter 2: introduces for the first time a model for inflation with light fields on an axion-dilaton system, with a new type of exact multi-field inflationary attractor that is true for both flat and curved field-space manifolds. Despite the fact that the inflaton trajectory is strongly turning, the isometry in the field space protects the dynamics of coupled inflationary perturbations, keeping the phenomenology to be single- field-like with negligible non-Gaussianity, as favoured by observations.

This chapter is based on [70]:
A. Achúcarro, E. J. Copeland, O. Iarygina, G. A. Palma, D. G. Wang and Y. Welling, *Shift-Symmetric Orbital Inflation: single field or multi-field?*, Phys. Rev. D **102**, no.2, 021302 (2020), [arXiv:1901.03657].

Chapter 3: investigates the viability of inflation with a spectator non-Abelian gauge field sector. We studied the theoretical restrictions for gravitational wave production dictated by the requirements for the gauge field to be in the spectator sector, as well as from the physics of the gauge sector itself. Such requirements result in the constraints for the amplitude and tensor tilt for chiral gravitational waves, and hence restrict the enhancement of the gravitational wave background with respect to the one coming from vacuum fluctuations.

This chapter is based on [86]:
O. Iarygina and E. I. Sfakianakis, *Gravitational waves from spectator Gauge-flation*, [arXiv:2105.06972].

- **Part II. Reheating in curved field spaces.**

Chapter 4: analytically demonstrates a competition between field-space and potential contributions that change the dynamics, duration and observable predictions of reheating for the multi-field α-attractors. We find universal scaling relations that allow for an easy estimate of the preheating efficiency for highly curved field geometries. Identification of important mass scales that control the tachyonic growth of fluctuations enables our work to take a first step towards an Effective Field Theory description of preheating in hyperbolic manifolds.

This chapter is based on [158]:
O. Iarygina, E. I. Sfakianakis, D. G. Wang and A. Achúcarro, *Universality and scaling in multi-field α-attractor preheating*, JCAP **06**, 027 (2019), [arXiv:1810.02804].

Chapter 5: provides an extensive study of the preheating behaviour for symmetric and asymmetric potentials about the minimum. We demonstrate the existence of a region in parameter space, where the symmetric and asymmetric multi-field α-attractors are explicitly not the same: one preheats and one does not. This leads to a different

cosmic history for the two models, with one possibly exhibiting a long matter-dominated phase, and a shift in the observational predictions for n_s and r.

This chapter is based on [159]:
O. Iarygina, E. I. Sfakianakis, D. G. Wang and A. Achúcarro, *Multi-field inflation and preheating in asymmetric α-attractors*, [arXiv:2005.00528].